

Pacific Northwest National Laboratory

Operated by Battelle for the
U.S. Department of Energy

Performance Assessment of the In-Well Vapor-Stripping System

T. J. Gilmore
M. J. Pinto
M. D. White
S. Ballard

S. M. Gorelick
O. Taban
F. A. Spane, Jr.

October 1996

RECEIVED

FEB 06 1997

OSTI

Prepared for the U.S. Department of Energy
under Contract DE-AC06-76RLO 1830

DISCLAIMER

This report was prepared as an account of work sponsored by an agency of the United States Government. Neither the United States Government nor any agency thereof, nor Battelle Memorial Institute, nor any of their employees, makes any warranty, express or implied, or assumes any legal liability or responsibility for the accuracy, completeness, or usefulness of any information, apparatus, product, or process disclosed, or represents that its use would not infringe privately owned rights. Reference herein to any specific commercial product, process, or service by trade name, trademark, manufacturer, or otherwise does not necessarily constitute or imply its endorsement, recommendation, or favoring by the United States Government or any agency thereof, or Battelle Memorial Institute. The views and opinions of authors expressed herein do not necessarily state or reflect those of the United States Government or any agency thereof.

PACIFIC NORTHWEST NATIONAL LABORATORY

operated by

BATTELLE

for the

UNITED STATES DEPARTMENT OF ENERGY

under Contract DE-AC06-76RLO 1830

Printed in the United States of America

Available to DOE and DOE contractors from the
Office of Scientific and Technical Information, P.O. Box 62, Oak Ridge, TN 37831;
prices available from (615) 576-8401.

Available to the public from the National Technical Information Service,
U.S. Department of Commerce, 5285 Port Royal Rd., Springfield, VA 22161



The document was printed on recycled paper.

DISCLAIMER

Portions of this document may be illegible in electronic image products. Images are produced from the best available original document.

Performance Assessment of the In-Well Vapor-Stripping System

T. J Gilmore
M. J. Pinto^(a)
M. D. White
S. Ballard^(b)
S. M. Gorelick^(a)
O. Taban^(c)
F. A. Spane, Jr.

October 1996

Prepared for
the U.S. Department of Energy
under Contract DE-AC06-76RLO 1830

Pacific Northwest National Laboratory
Richland, Washington 99352

(a) Stanford University
(b) Sandia National Laboratories
(c) Earth Technology Corporation

MASTER

DISTRIBUTION OF THIS DOCUMENT IS UNLIMITED

W

Summary

In-well vapor stripping is a remediation technology designed to preferentially extract volatile organic compounds dissolved in groundwater by converting them to a vapor phase and then treating the vapor. This vapor-stripping system is distinctly different from the more traditional in situ air-sparging concept. In situ sparging takes place in the aquifer formation; in-well vapor stripping takes place within the well casing.

The system was field demonstrated at Edwards Air Force Base, California; the first-time demonstration of this technology in the United States. Installation and testing of the system were completed in late 1995, and the demonstration was operated nearly continuously for 6 months (191 days) between January 16 and July 25, 1996. Postdemonstration hydrochemical sampling continued until September 1996.

The demonstration was conducted by collaborating researchers from Pacific Northwest National Laboratory^(a) and Stanford University as part of an interim cleanup action at the base. Edwards Air Force Base and its environmental subcontractor, Earth Technology Corporation, as well as EG&G Environmental, holders of the commercial rights to the technology, were also significant contributors to the demonstration.

Edwards Air Force Base was chosen for the demonstration because of both their willingness to host the demonstration and because of its existing hydrogeologic database. The selected site met the initial criteria for a demonstration — volatile organic contamination in the groundwater, no co-contamination in the vadose zone, suitable hydraulic conductivities, and low hydraulic gradient. Additional site-specific information was collected for planning and design of the demonstration. In general, the characterization data indicated the site geology was very heterogeneous, varying, both laterally and vertically. The heterogeneity of the site had a large influence on the cleanup zone of the system.

The in-well vapor-stripping system was successful in significantly reducing the concentration of trichloroethylene (the contaminant of concern) in the groundwater. The zone of influence defined by the trichloroethylene reduction was at least a 50-ft radius in the upper zone of the aquifer and at least a 10-ft radius and possibly greater than a 30-ft radius in the lower zone.

This asymmetrical cleanup zone is the result of the geologic heterogeneities at the site. The contaminant was reduced by nearly 2 orders magnitude to below the regulatory limit of 5 $\mu\text{g/L}$ in the shallow zones of the aquifer. An ~40% reduction (290 to 173 $\mu\text{g/L}$) of trichloroethylene was measured in the lower zones of the aquifer. The stripping ratio of the system averaged 90%; that is, 90% of the contaminant was removed per pass through the system.

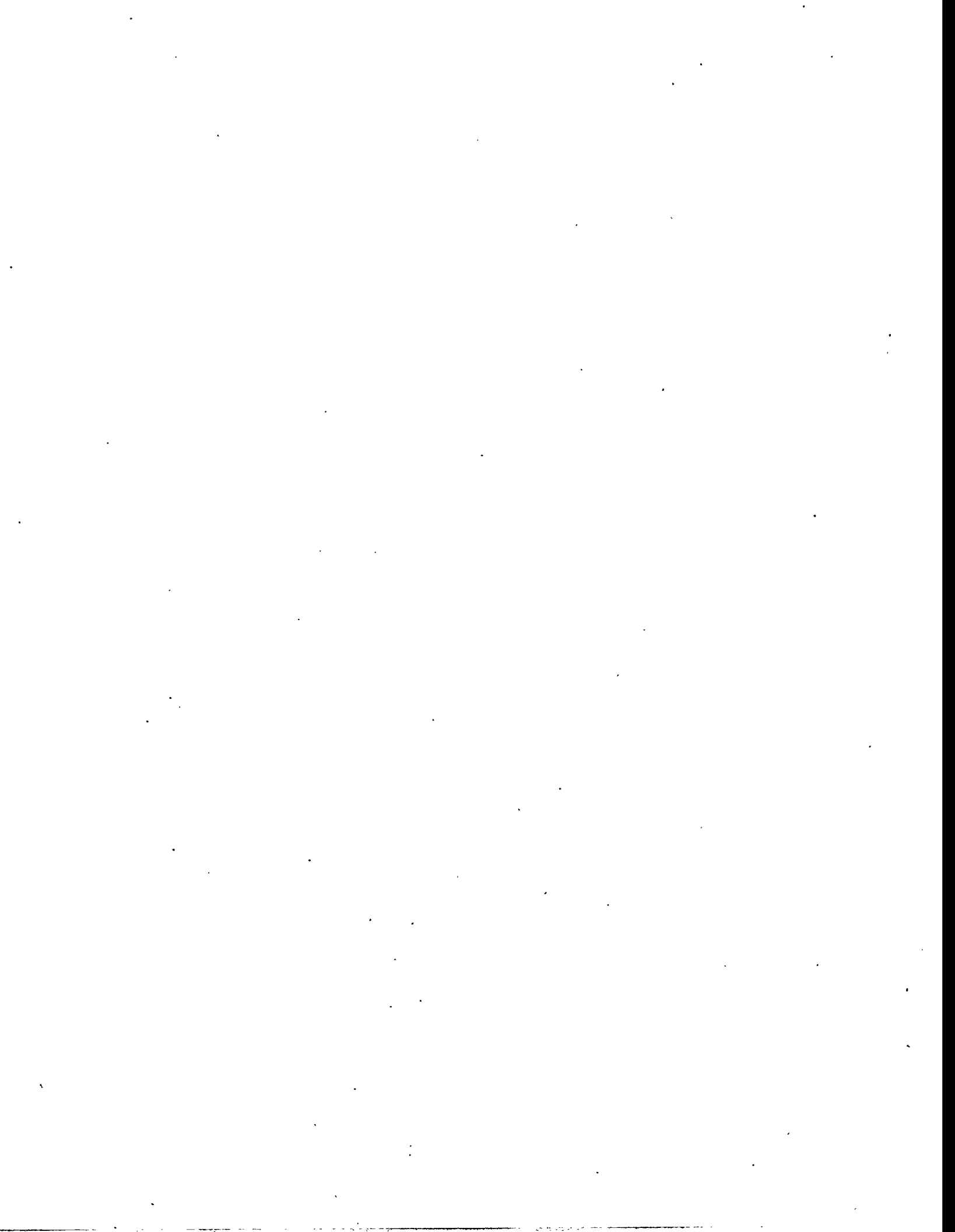
(a) Pacific Northwest National Laboratory is operated by Battelle for the U.S. Department of Energy.

A number of refinements were made for better use of the system during the demonstration: substituting blowers for the air compressor, adding an eductor pipe, maximizing and maintaining the infiltration rates of the upper zone by periodically adding calcium to the system, fully developing the lower pumping zone, controlling organic and inorganic precipitation by running the system in a closed loop and adding carbon dioxide to maintain proper pH, and controlling condensation effects in the aboveground system apparatus.

The system proved both efficient and effective in removing the contaminant from the aquifer.

Acknowledgments

This field demonstration of the in-well vapor-stripping system was funded by the U.S. Department of Energy (DOE's) Office of Technology Development (EM-50) and the Environmental Management Office of the Air Force Flight Test Center. Mr. Thomas Brouns, the Plumes Focus Area's Volatile Organic Compounds Product Line Manager, provided the support and guidance needed to complete the DOE-funded portion of the demonstration. Mr. David Steckel and the Environmental Management Office at Edwards Air Force Base provided support for the United States Air Force's portion of the demonstration. Earth Technology Corporation, as the Edwards Air Force Base prime environmental contractor, provided essential field support. EG&G Environmental provided equipment and technical advice, and Sandia National Laboratories provided the in situ flow sensors as part of the overall demonstration.



Contents

Summary	iii
Acknowledgments	v
1.0 Introduction	1.1
2.0 Technology Description	2.1
3.0 Field Test Objectives and Approach	3.1
3.1 Approach	3.1
4.0 Demonstration Site	4.1
4.1 Site Selection	4.1
5.0 Design and Evaluation Tools	5.1
5.1 Treatment Well Design Optimization	5.1
6.0 Monitoring Network	6.1
6.1 Demonstration Wells	6.1
6.2 Monitoring Wells	6.1
6.3 Piezometers	6.3
6.4 Flow Sensors	6.6
6.5 Characterization Wells	6.7
6.6 CERCLA Monitoring Wells	6.7
7.0 Site Characteristics	7.1
7.1 Stratigraphy	7.1
7.2 Groundwater	7.2
7.3 Surfacewater	7.2
7.4 Soil Chemistry	7.4

7.5	Water Chemistry	7.4
7.6	Contaminant of Concern	7.4
8.0	Methods	8.1
8.1	Water-Flow Rate	8.1
8.1.1	Downhole Weir	8.1
8.1.2	Orifice Plate	8.1
8.1.3	Empirical Operating Curves	8.3
8.1.4	Recharge Rate	8.3
8.2	Off-Gas Readings	8.3
8.3	Groundwater Velocity Measurements	8.5
8.4	Groundwater Parameters	8.5
8.5	Groundwater Sampling	8.5
8.6	Lithologic Sampling	8.5
9.0	Design of Aboveground Apparatus	9.1
9.1	Treatment Trailer	9.1
9.2	System Control and Data Logging	9.1
10.0	System Optimization and Refinements	10.1
10.1	Blowers Versus Air Compressor	10.1
10.2	Controlling System pH	10.1
10.3	Infiltration/Reinfiltration	10.3
10.4	Use of Eductor Pipe to Optimize Pumping Rates	10.4
10.5	Closed-Loop System	10.4
10.6	Condensation Effects	10.5
11.0	Performance Data	11.1

11.1	Concentration Trends in Monitoring Wells	11.1
11.2	Zone of Influence	11.4
11.2.1	Recirculation	11.4
11.3	Pumping Rates	11.6
11.4	Airflow Rates and Stripping Ratio	11.8
11.4.1	Theoretical Stripping Rates	11.8
11.5	Groundwater Mound Development from Recharge	11.10
11.6	Postdemonstration Concentration Trends	11.12
11.7	In Situ Permeable Flow-Sensor Results	11.14
12.0	Conclusions	12.1
13.0	References	13.1

Figures

1.1	Location Map	1.2
2.1	In-Well Vapor-Stripping System	2.2
4.1	Demonstration Site Location	4.2
5.1	Well Design Options for Field Demonstration	5.2
5.2	Pond Height Versus Pumping/Infiltration Rate	5.3
6.1	Monitoring Well Network	6.2
6.2	Perspective View of Monitoring Network	6.3
6.3	Demonstration Well Construction	6.4
6.4	Monitoring Well Construction	6.5
6.5	Piezometer Construction	6.6
7.1	Geologic Cross Section of Demonstration Site	7.3
7.2	Dispersive Clay Zonations	7.5
8.1	Down-Well Water-Flow Meter	8.2
8.2	Operating Curves Using a 400-Micron Sparger Element	8.4
9.1	Treatment Trailer	9.2
9.2	Interactive Computer Screen	9.3
10.1	System Operation Reflected by Flow-Sensor Data at F3	10.2
11.1	Trichloroethylene Concentrations in Shallow Monitoring Wells	11.2
11.2	Trichloroethylene Concentrations in Deep Monitoring Wells	11.3
11.3	Concentration Profiles for Estimating Recirculation	11.7
11.4	Intake and Outflow Concentrations with Stripping Ratios	11.9
11.5	Piezometer Water Levels	11.11

11.6	Shallow Monitoring Well TCE Concentrations Versus Elapsed Time	11.12
11.7	Deep Monitoring Well TCE Concentrations Versus Elapsed Time	11.13
11.8	Flow Velocity as a Function of Time Observed by Flow Sensor F3	11.15
11.9	Flow Velocity as a Function of Time Observed by Flow Sensor F2	11.16
11.10	Flow Velocity as a Function of Time Observed by Flow Sensor F1	11.17
11.11	Measured Flow-Velocity Vectors	11.18
11.12	Horizontal Components of Flow Velocities Measured by Three Flow Sensors after Subtraction of Background Flow Velocities	11.19

Tables

3.1	Parameters Measured During Demonstration	3.2
7.1	Summary of Site Characteristics	7.1
11.1	Recirculation Rates	11.7
11.2	Comparison of Measured and Theoretical Stripping Rates	11.9

1.0 Introduction

The in-well vapor-stripping system is an in situ remediation technology designed to preferentially extract volatile organic compounds (VOCs) dissolved in groundwater by converting them to a vapor phase and treating the vapor. The concept was initially proposed by researchers at Stanford University (Gvirtzman and Gorelick 1992). The U.S. Department of Energy supported the concept and provided funding for testing the concept and bridging the gap to application. A vapor-stripping well was first built and tested in the laboratory at the U.S. Department of Energy's Hanford Site through a collaboration between Stanford University and Pacific Northwest National Laboratory (Gilmore and Francois 1996; Francois et al. 1996). Following the successful demonstration of the system in the laboratory, a field demonstration was planned. Although the field demonstration was originally slated for the Hanford Site, because of budgetary and field constraints, the system was installed at Edwards Air Force Base (AFB) in Southern California during the summer of 1995.

The installation of this technology at Edwards AFB (Figure 1.1) was the first demonstration of a system of this kind in the United States. One other system completed operation in France, and additional vapor-stripping systems are scheduled at the time of this report.

The commercial rights to the system were purchased in late 1995 by EG&G Environmental, Pittsburgh, Pennsylvania, from Stanford University, who holds the patent rights. Because the system is a patented technology, a license is required for its operation. An educational license was granted to Edwards AFB by Stanford University to demonstrate this technology at the base. The system is available for commercial applications through EG&G Environmental under the name NoVOCs.

This report gives the detailed description of the field demonstration that was conducted at Edwards AFB. A description of the technology is given in Chapter 2.0, the objectives and approach in Chapter 3.0, an overview of the demonstration site in Chapter 4.0, a discussion of the design and evaluation in Chapter 5.0, the details of the monitoring network in Chapter 6.0, and the site characteristics in Chapter 7.0. The methods used in the determination of the various parameters are given in Chapter 8.0. Chapter 9.0 gives the design of the aboveground apparatus. The system optimization discussion is provided in Chapter 10.0. Performance data are given in Chapter 11.0, followed by the conclusions in Chapter 12.0. The references cited in the text are last, in Chapter 13.0.

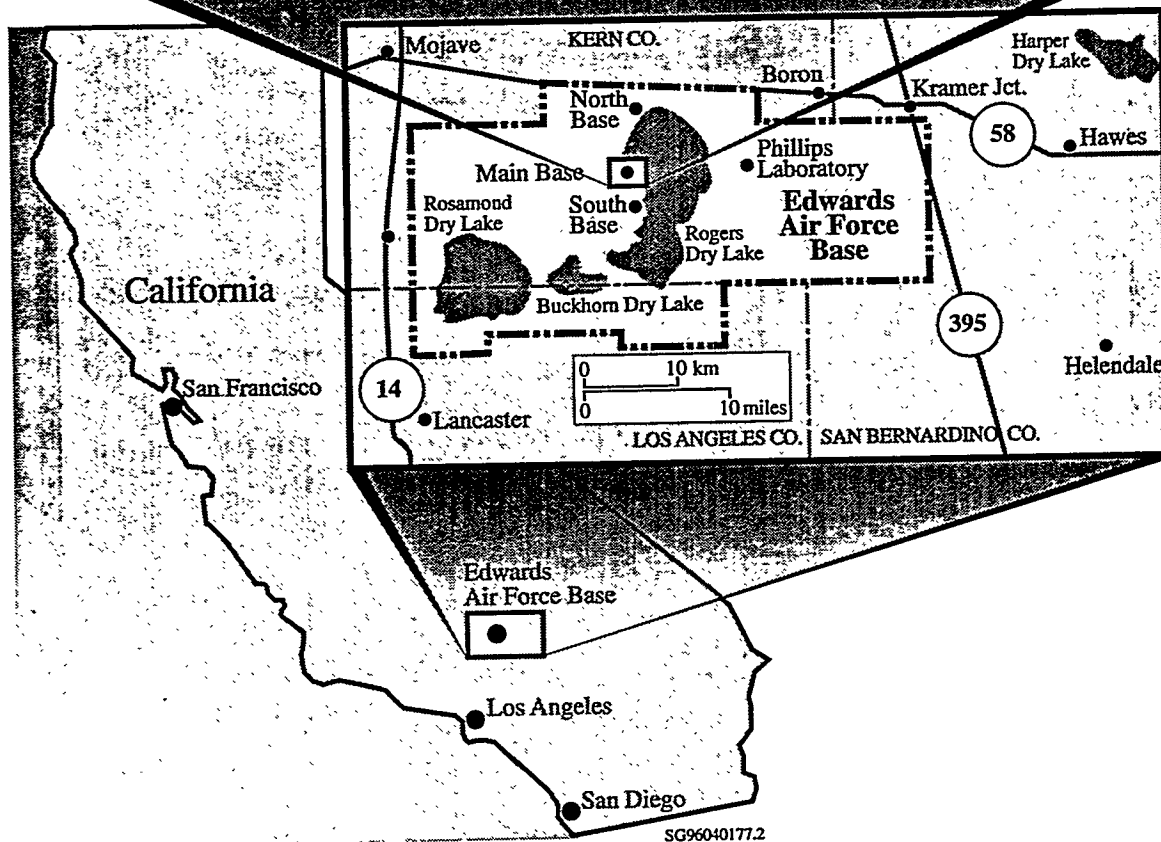
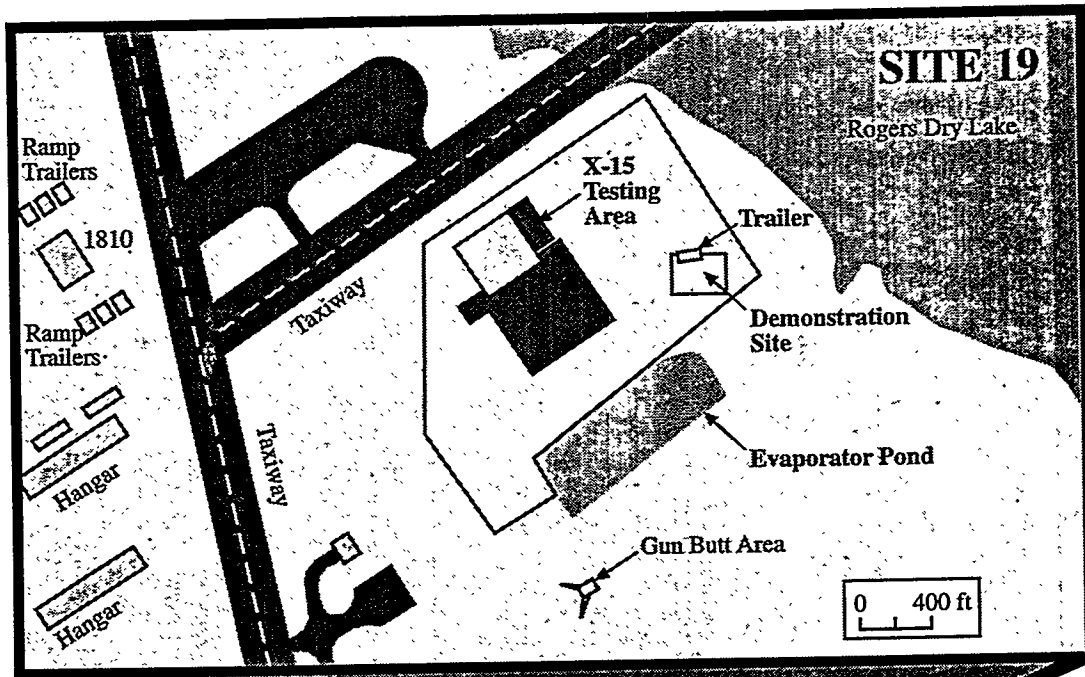
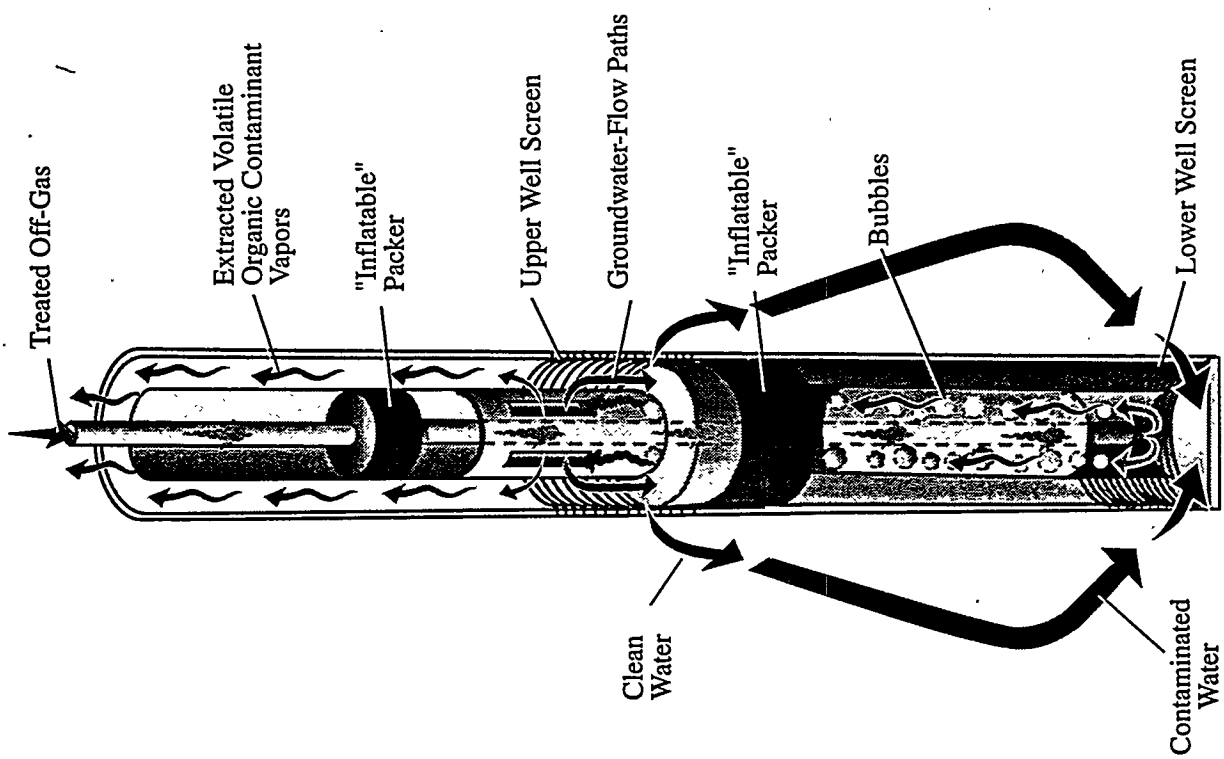


Figure 1.1. Location Map

2.0 Technology Description

The in-well vapor-stripping system is designed to extract VOCs dissolved in groundwater without removing or treating water above the ground (Figure 2.1). It is an in situ system that works by converting VOCs to a vapor phase in the well and then drawing off the vapor for treatment above the ground. Airlift pumping is used to aerate and lift the groundwater within the well. The aeration strips dissolved VOCs from the aqueous phase into the gas phase, and the lifting moves the aerated water in the well to a zone above the water table. The treated water is released into the vadose zone through a screened portion of the well and allowed to infiltrate back to the water table. By simultaneously extracting groundwater and by reintroducing water above the water table, a circulation cell is created in the subsurface that systematically removes the VOCs.

This technology is distinctly different from the more traditional in situ air sparging (Johnson et al. 1993), in which air is injected into water-saturated sediments, in that it strips VOCs from the groundwater within the borehole.



S96040177.8

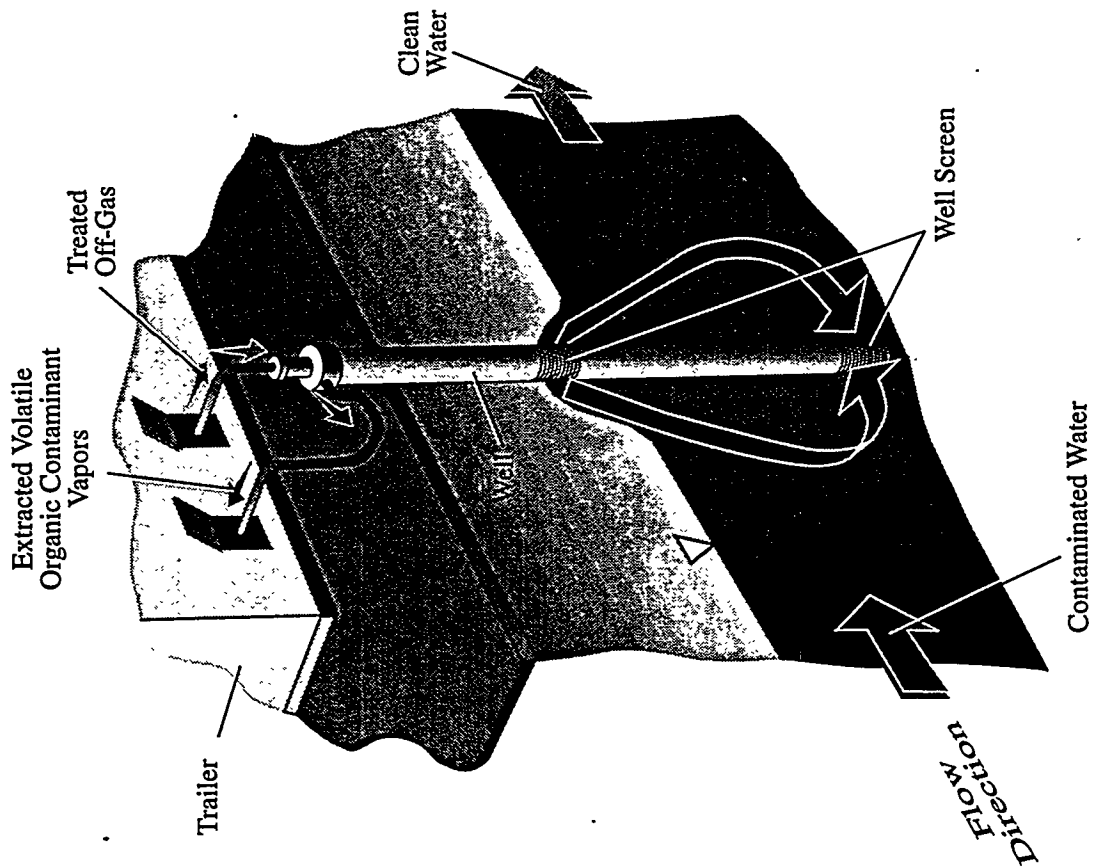


Figure 2.1. In-Well Vapor-Stripping System

3.0 Field Test Objectives and Approach

The primary objective of the field demonstration was to determine the system's effectiveness in removing VOCs from groundwater. The data collected were focused on reaching this determination. Based on predemonstration estimates, the system would be considered successful if the contaminant concentration in the downgradient well were reduced by 60% or greater. Additional objectives identified in part through stakeholder involvement included the following:

- optimizing system operation
- determining radius of influence
- identifying system effects on the subsurface
- determining level of cleanup attainable
- comparison to baseline technology (pump and treat)
- cost to operate.

The data collected during the demonstration to support the objectives are presented in Table 3.1. This report uses the available data to address the objectives; however, some of the objectives, such as the cost to operate the system and the comparison to pump and treat, are not included in this report and should be obtained from the commercial vendor for the technology, EG&G Environmental, Pittsburgh, Pennsylvania.

The program under which this technology was developed, the Volatile Organic Compounds in Arid Soils Integrated Demonstration (VOC-Arid ID), extensively involved stakeholders in the evaluation of its Hanford Site-directed remediation technologies (Peterson et al. 1995). Stakeholders are groups and individuals with an interest in cleanup, including regulatory agencies, Native American tribes, environmental and civic-interest groups, public officials, environmental technology users, and private citizens. The stakeholders' input validated the technology evaluation criteria and helped to identify the secondary objectives.

3.1 Approach

The overall approach to testing and evaluating the in-well vapor-stripping concept was a phased approach. The system was first tested in the laboratory. The laboratory work provided the proof-of-principle of the system, as well as system refinements, operational parameters, and testing and building of some of the field components. The complexity of the natural environment required that the first demonstration of the system be limited to a single treatment or demonstration well surrounded by an

Table 3.1. Parameters Measured During Demonstration

Parameter	Source	Method	Data Use	Rate
Volatile organic compound (VOC) off-gas concentrations	Outlet air line at well head	Infrared photoacoustic spectrometer	Mass-balance calculation/optimize system	Continuous
Carbon dioxide off-gas concentrations	Outlet air line at well head	Infrared photoacoustic spectrometer	Control pH in circulation water	Continuous
VOC water concentrations in aquifer	Monitoring wells	SW846 (8010/8020) EPA (1986)	Monitor concentration trends around treatment well	1 per week
Groundwater parameters (dissolved oxygen, temperature, pH)	Monitoring wells, treatment well	Hydroprobe	Monitor parameter trends around treatment well	1 per day
VOC circulation water concentrations in demonstration well	Water entering and exiting treatment well	SW846 (8010/8020) EPA (1986)	Mass-balance calculation/determine stripping rate	1 per week
Pressure-head measurements in aquifer	Measure in monitoring wells	Pressure transducer	Equipment optimization/flow-cell determination	Continuous
Water-mounding height	1-in. piezometers	Steel tape	Characterize groundwater mound development	Periodic
Groundwater velocities in aquifer	In situ flow sensor	Thermal perturbation	Characterize flow cell	Continuous
Inlet airflow rate	Inlet air line at head of eductor pipe	Flow meter	Equipment optimization	Continuous
Exhaust airflow rate	Outlet air line at well head	Flow meter	Equipment optimization	Continuous
Temperature of inlet air	Inlet air line at head of eductor pipe	Thermocouple wire	Mass-balance calculation	Continuous
Temperature of outlet air	Outlet air line at well head	Thermocouple wire	Mass-balance calculation	Continuous
Pressure/injection rate of inlet air	Inlet air line at head of eductor pipe	Pressure transducer	Equipment optimization	Continuous
Pressure of outlet air	Outlet air line at well head	Pressure transducer	Equipment optimization	Continuous
Groundwater pumping rate	Downhole flow meter	Pressure transducer	Equipment optimization/computer simulations, treatment rate	Continuous
	Recharge test	Measuring bucket		Periodic

extensive monitoring network. It also required that the field activities be conducted in stages. Each stage was designed to supply the data necessary to design subsequent phases. The major activities in the approach included the following:

- obtaining background site information
- obtaining site-specific information by drilling two characterization wells for sediment sampling and aquifer testing
- evaluating results of the characterization phase to determine if the site were suitable for demonstrating the system and, if so, beginning the design of the system and monitoring network
- installing demonstration well and monitoring well network
- reevaluating data and well construction, which necessitated installing a second treatment well
- establishing baseline for groundwater chemistry and flow conditions
- testing equipment
- operating system for demonstration
- monitoring after experiment
- analyzing and reporting data.

It should be noted that this approach was designed for demonstrating a new technology, and it is not expected that this extensive approach would be required for commercial technology applications. For example, the number and type of monitoring points around the treatment well were much more extensive than the number and type that would be required for the effective application of the technology.

This report gives all units of measurement in the form they were recorded. For accuracy of interpretation and use by others in the industry, no English or metric conversions are given. Unit conversions are available in *American Society for Testing and Materials* (1994).

4.0 Demonstration Site

The demonstration site is located at Edwards AFB, California ~60 mi northeast of Los Angeles at the western edge of the Mojave Desert (see Figure 1.1). The primary use of the base is for aircraft research, development, and testing programs. The base was listed on the National Priorities List for cleanup under the Comprehensive Environmental Response, Compensation, and Liability Act of 1980 (CERCLA) and was divided into 10 operable units based primarily on location at the base. The demonstration site for the system is located in Operable Unit 1, Site 19 (Figure 4.1). Groundwater beneath the demonstration site is contaminated with dissolved volatile organics, primarily trichloroethylene (TCE). The contamination is believed to have resulted from the disposal of TCE to the ground after the cleaning of experimental rocket planes in the 1960s and 1970s. This demonstration was conducted as an interim cleanup action as part of the CERCLA process at the site.

4.1 Site Selection

The demonstration site was selected using several criteria, including availability of hydrogeologic data on the area, presence of VOC contamination in the aquifer, no known co-contamination in the vadose zone, good hydraulic conductivities, and a low hydraulic gradient. However, to make the final selection of the site, additional site-specific data were collected from drilling two characterization wells at the proposed demonstration site (see wells on Figure 4.1):

- detailed geologic sampling to identify any low-permeability zones
- additional aquifer testing to more accurately determine the vertical hydraulic conductivity and to verify horizontal hydraulic conductivities
- additional sampling to verify there were no co-contaminants within the projected zone of influence.

The results from this additional characterization phase, used in conjunction with previous investigations, identified two areas of concern for demonstrating the technology at this site: two zones of relatively low hydraulic conductivity (one near the water table at 29 ft and one at ~44 ft). The regional hydraulic conductivity was also low but within the range specified for demonstrating the system. The decision was made to use the selected site and to further evaluate the two low-permeability zones. The results of the investigations are summarized in the discussion of site characteristics (Chapter 7.0).

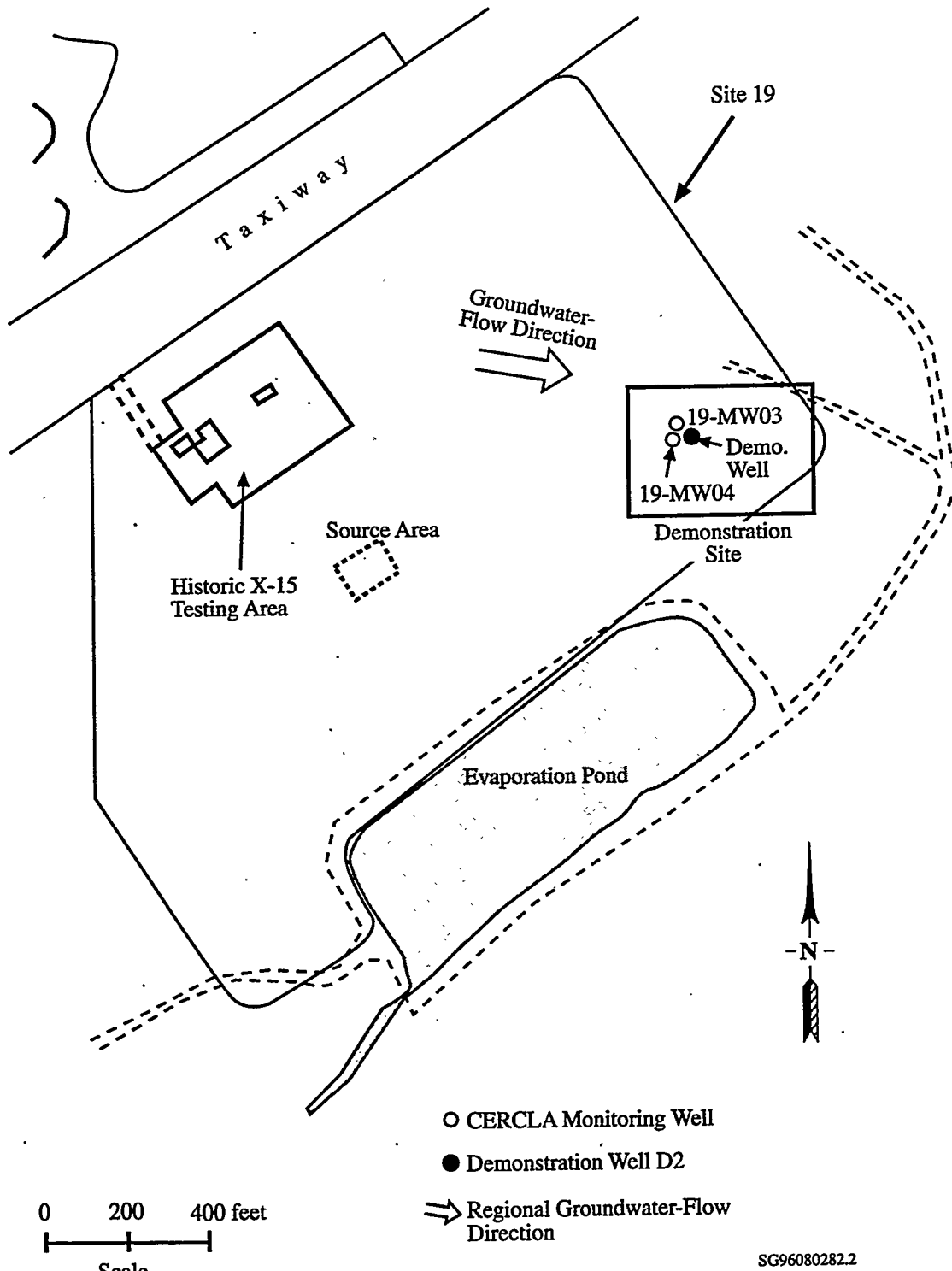


Figure 4.1. Demonstration Site Location

5.0 Design and Evaluation Tools

Several design tools were used and developed during the demonstration, one of which was a model for airlift pumping (Francois et al. 1996). This model was developed as a result of the laboratory testing done for the design and substantiation of field results during the demonstration. In addition to the airlift model, an interactive spreadsheet was developed to aid in the design of the system.

The primary computer code used in these simulations was the Subsurface Transport Over Multiple Phase (STOMP) simulator (White et al. 1995). STOMP is capable of simulating a large variety of subsurface transport problems involving the flow of water, air, VOC, energy, and dissolved solutes over multiple phases. The simulator design is based on a variable source code configuration, which constructs the source code in response to the problem specifics.

Numerical simulations of the in-well vapor-stripping system were used to design the layout of monitoring equipment, predict system performance, and visualize operational characteristics (White and Gilmore 1996). Monitoring equipment design and system performance predictions with numerical simulations were completed prior to field operation of the system based on estimates of hydraulic properties from grain-size distributions, porosity measurements, and permeability tests. The simulator was also used to interpret the results during and following the demonstration. The results are included in the performance data (Chapter 11.0). The conceptual model development can be found in White and Gilmore (1996).

5.1 Treatment Well Design Optimization

The pumping capacity of the system depends on the performance of the airlift process and infiltration capacity. The airlift operation and performance vary with total lift and submergence of the air line below the pumping level. Infiltration capacity is dependent on the saturated conductivity of the sediments between the extraction and infiltration intervals and the distance of the infiltration interval above the static water-table height. A principal design parameter for the system, therefore, is the length and spacing of the upper and lower screened intervals. Five design options were considered for the demonstration, shown in Figure 5.1 as well designs A through E. Pumping/infiltration capacity predictions were generated for each well design using the STOMP simulator with the conceptual model.

Simulations to determine pumping/infiltration capacity were initialized with a static hydraulic gradient for zero-recharge conditions and executed for a simulation period of 100 days, sufficient time to reach steady-state conditions. Steady-state results from the pumping/infiltration capacity simulations for the five system designs are shown in Figure 5.2. These results show two regimes for the ponding-height versus pumping-rate relationship. Ponding height is the height that water backs up inside the infiltration screen before moving into the formation sediments. For ponding heights within the upper screened interval, a nonlinear relationship occurs between the ponding height and the pumping rate.

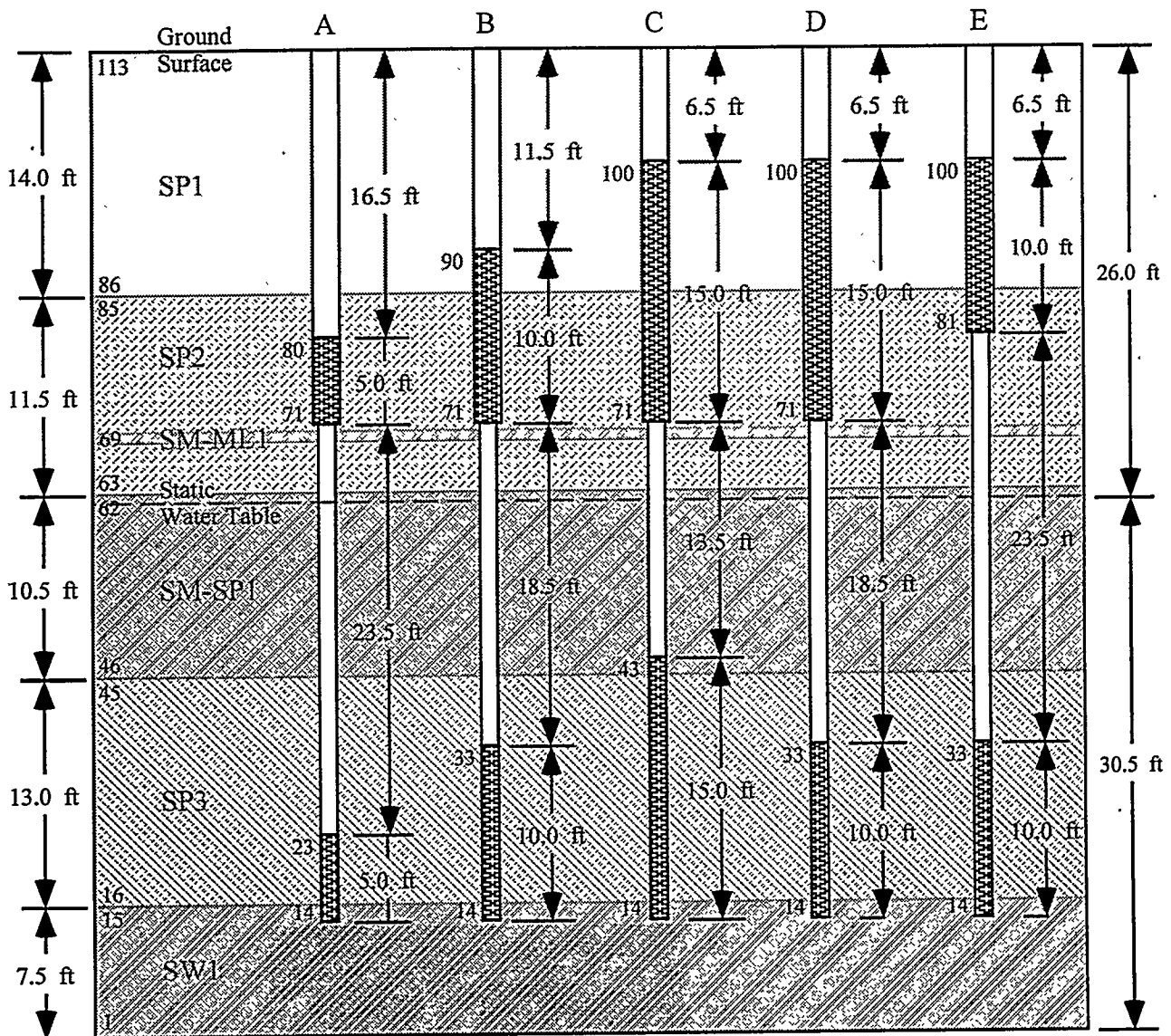


Figure 5.1. Well Design Options for Field Demonstration

This nonlinear relationship results from the proportional change in infiltration area from the upper screened interval with ponding height. For ponding heights greater than the upper screened interval, a nearly linear relationship occurs between the ponding height and the pumping rate. For this demonstration, pumping/infiltration capacity appears generally to be limited by ponding heights or infiltration rates of the system. Comparison of designs B and E demonstrates the benefit of raising the height of the upper screened interval above the static water-table level in terms of ponding. For the demonstration at Edwards AFB, design D was used. The objective was to raise the height of the screened interval as far above the water table as reasonable while still maximizing the infiltration area by using a

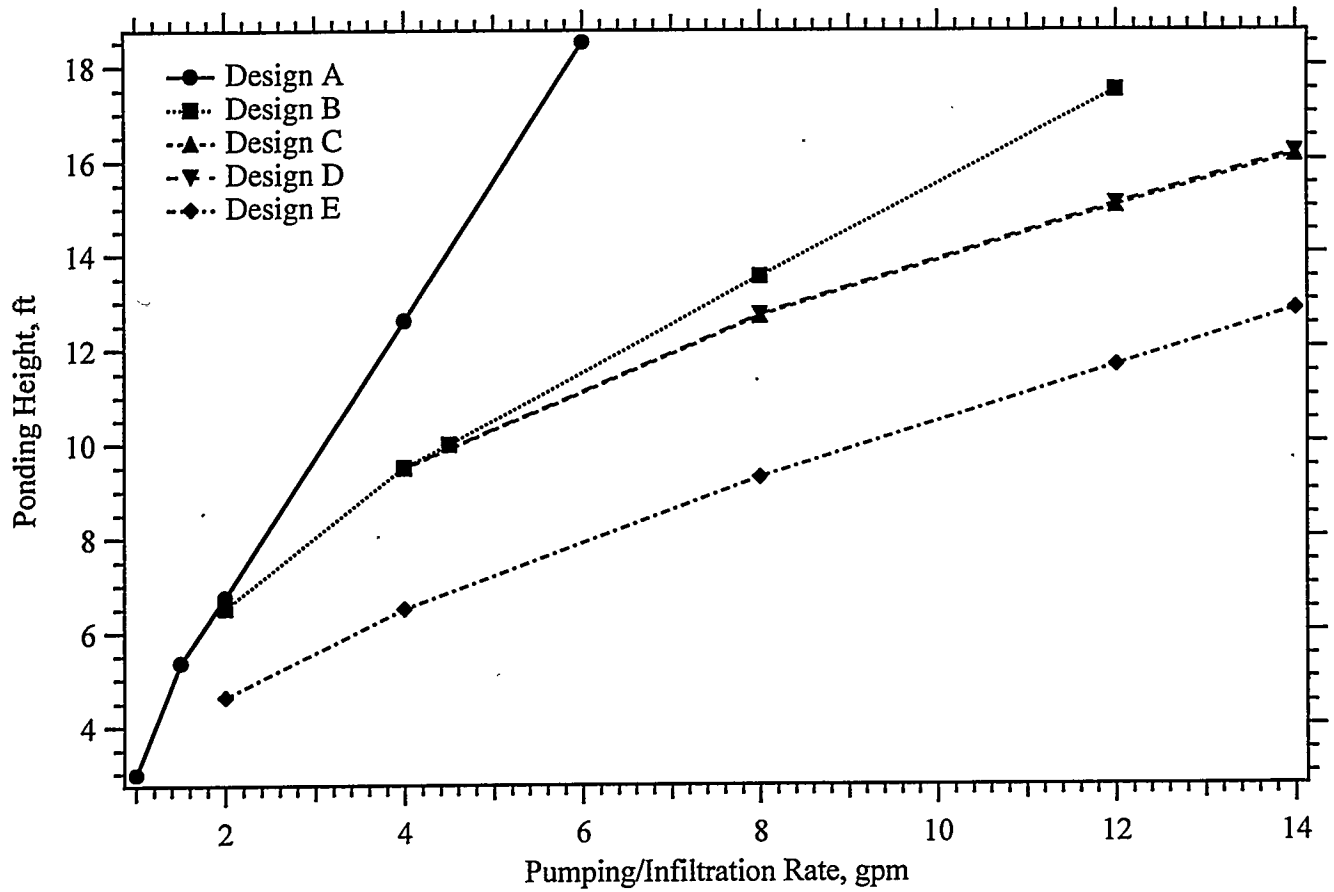


Figure 5.2. Pond Height Versus Pumping/Infiltration Rate

longer screen. The upper screen was 15 ft long and placed ~7 ft above the water table. The intake screen was 10 ft long and placed at the bottom of the aquifer to increase the screen separation.

6.0 Monitoring Network

The monitoring network consists of a demonstration or treatment well with associated access tubes, five dual-completion monitoring wells, three piezometers, three flow sensors, two characterization wells, and two older monitoring wells drilled during the remedial investigation of Site 19 (Figures 6.1 and 6.2).

6.1 Demonstration Wells

The demonstration well is the vapor-stripping well where the groundwater treatment takes place and is the center of the monitoring network. Two "demonstration" wells were constructed (D1 and D2); however, D1 was never used for groundwater treatment. The primary demonstration well was D2. Although D1 was not used for treatment, it was used for monitoring and infiltration testing.

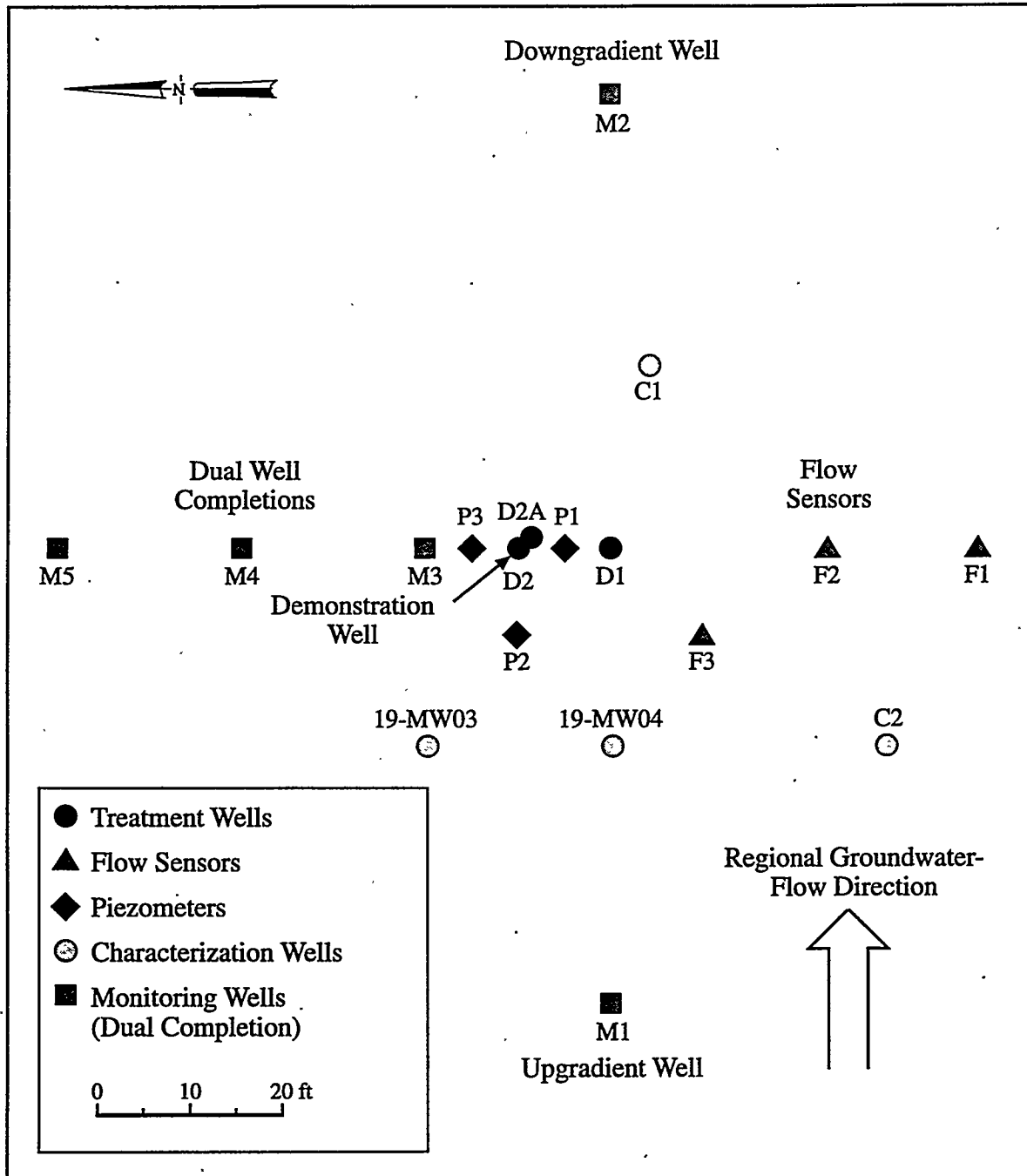
Well D1 was completed with 10-in. casing from just above ground surface to 50 ft below ground surface. Two screens were installed; the lower screen between 30 and 50 ft and the upper screen between 3 and 18 ft below the surface (Figure 6.3[a]). Well D2 was completed with 6-in. casing to 50 ft below ground surface, with a screened interval between 40 and 50 ft. Ten-inch casing was placed in the ground to a depth of 20 ft (Figure 6.3[b]). The upper screened interval was placed between 3 and 18 ft below ground surface, providing a screened separation of ~22 ft, or 10 ft more than in well D1. A bentonite seal isolates the upper and lower screened intervals in each well. Well D2a is a 2-in. access tube that was completed between 45 and 50 ft within the same borehole as well D2. This access tube allows monitoring of the lower intake zone of well D2.

The well was later modified with a 4-in. eductor pipe replacing the 6-in. casing. The 6-in. casing was extracted from just above the end of the 10-in. casing at ~20 ft and a packer was placed between the 4-in. and 6-in. casings near that point.

6.2 Monitoring Wells

A total of five monitoring wells (M1 through M5) were constructed to be used for sampling and pressure-head measurements. Each monitoring well is identical in design, and each monitors the top and bottom of the upper unconfined aquifer. There are 2 casing strings of 2-in.-dia. stainless steel in each borehole (M1s [shallow], M1d [deep], etc.). The deep casing is screened between 45 and 50 ft below ground surface at the bottom of the aquifer, and the shallow casing is screened between 30 to 35 ft below ground surface near the top of the aquifer. A bentonite seal isolates the two completion zones in the borehole (Figure 6.4).

The monitoring wells were located away from the treatment wells as follows: well M1 was placed 50 ft upgradient; M2 50 ft downgradient; M3 10 ft crossgradient; M4 30 ft crossgradient; and M5 50 ft crossgradient. The positioning of these wells was based on computer simulations of the predicted zone



SG96040177.7

Figure 6.1. Monitoring Well Network

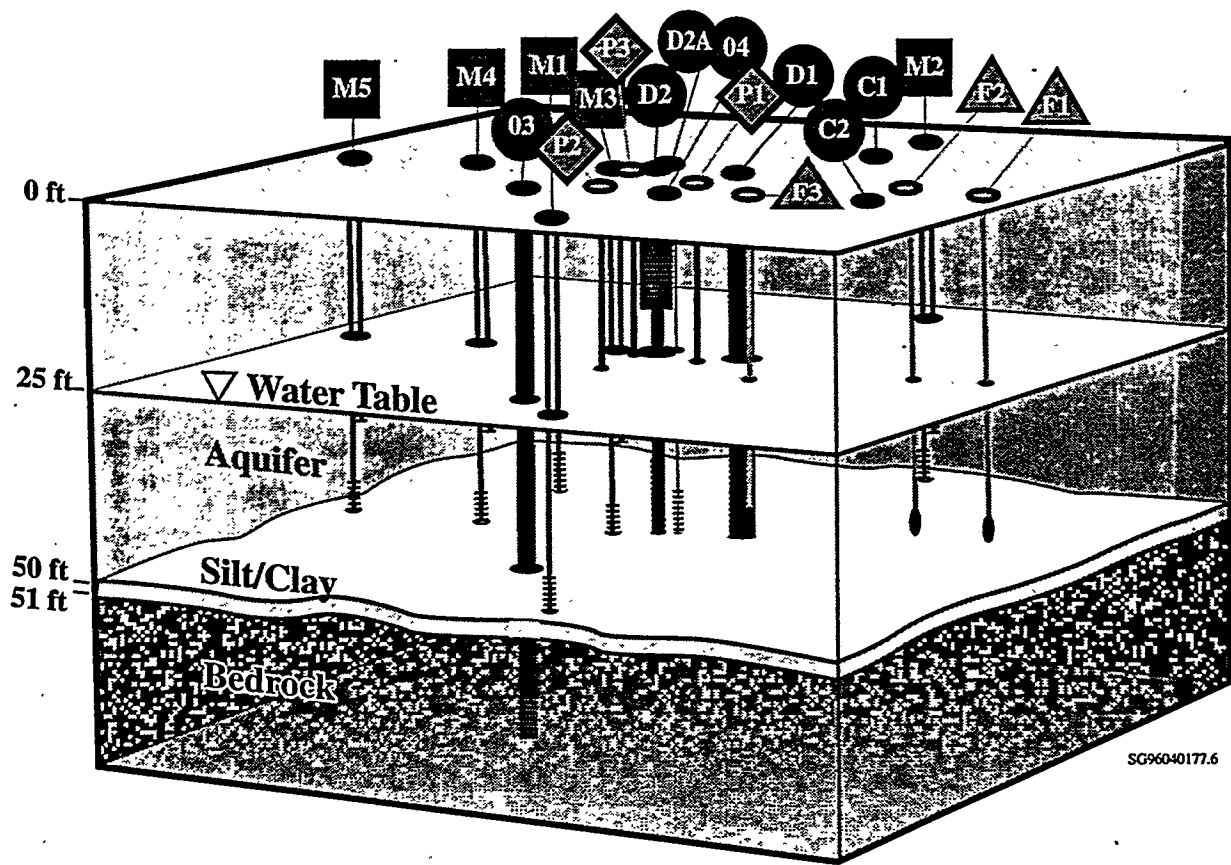


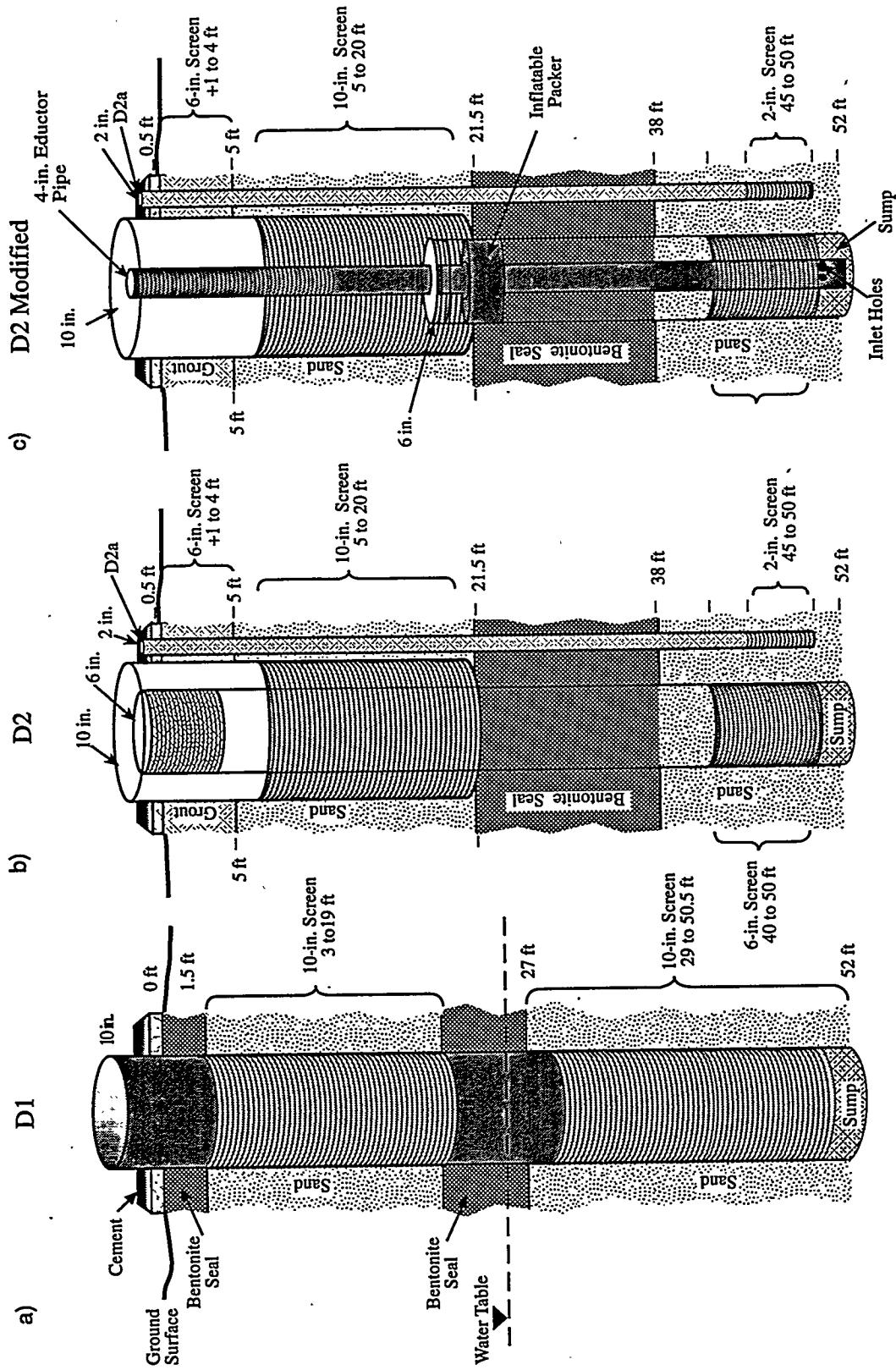
Figure 6.2. Perspective View of Monitoring Network

of influence. Well M2, the downgradient well, is considered "the-point-of-compliance" well. If contamination concentrations decline in this well, the vapor-stripping system would be considered effective. All monitoring wells were drilled using the air-rotary method.

6.3 Piezometers

The piezometers were used to monitor the groundwater mound as it developed around the treatment well as a result of the reinfiltrating water.

A total of three piezometers (P1, P2, and P3) were constructed using heavy-gauge, 1-in.-dia. steel tubing with a drive point on the bottom. The piezometers were "pushed" into the ground using a casing hammer and/or hydraulically pushed using the drill head on an auger rig. The piezometers have a 1-ft-long screen at the end of the steel pipe and were completed ~1 ft into the aquifer at 28 ft (Figure 6.5).



SC96080282.1

Figure 6.3. Demonstration Well Construction

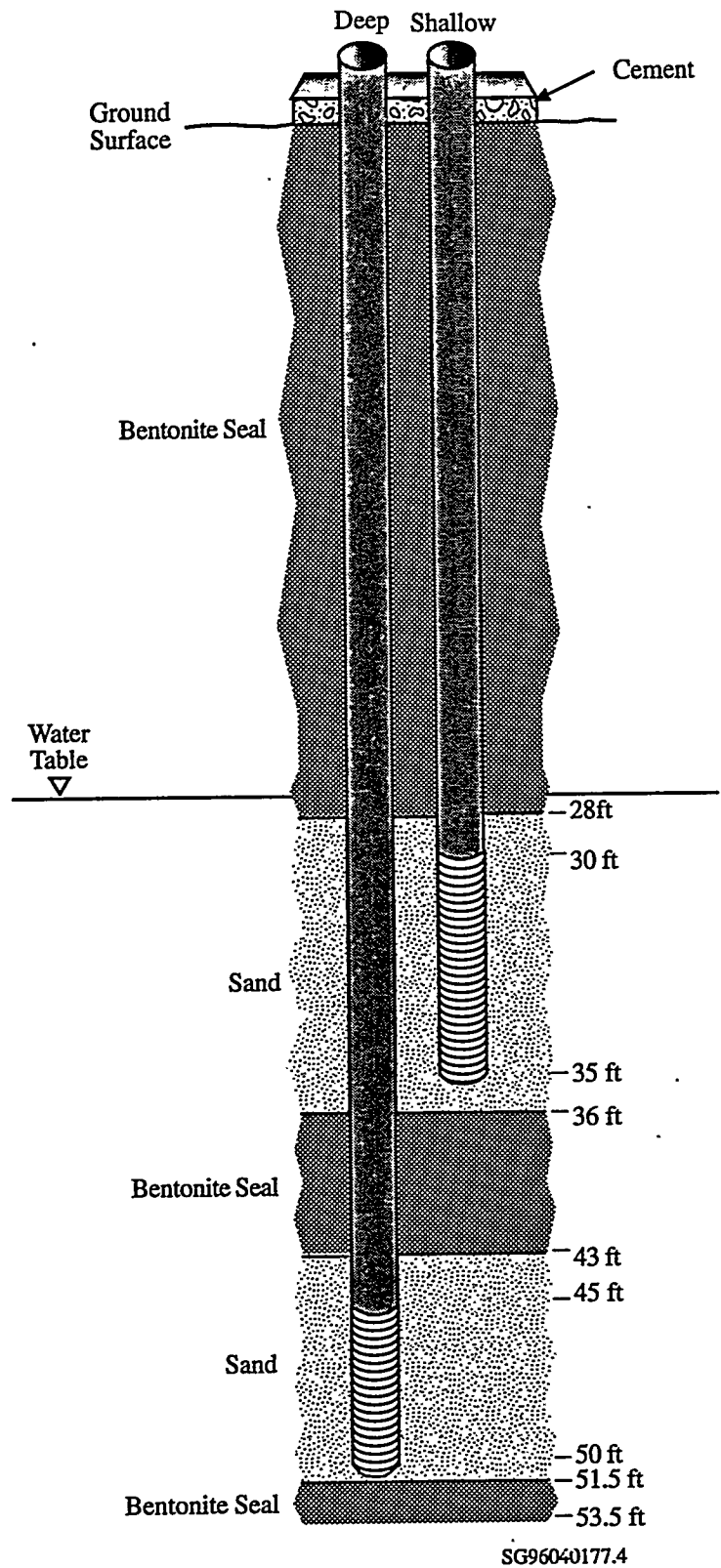
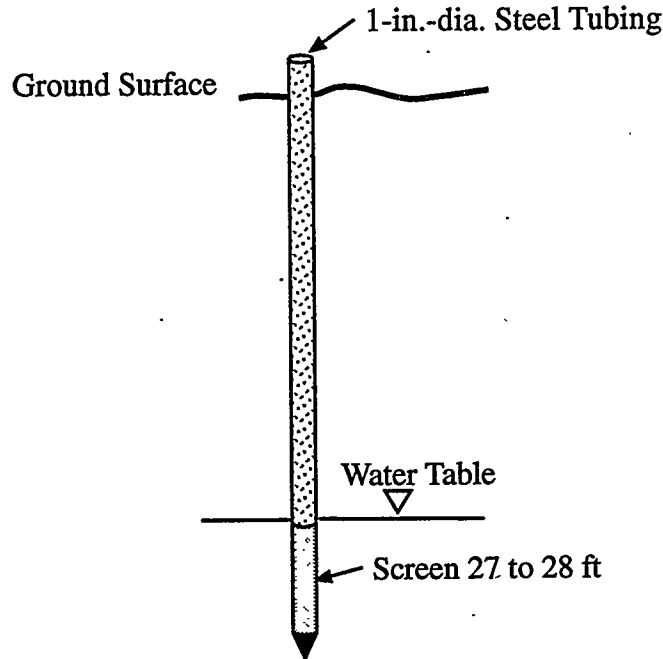


Figure 6.4. Monitoring Well Construction



SG96080282.3

Figure 6.5. Piezometer Construction

Piezometer P1 is located 5 ft crossgradient of the treatment well to the south, P2 is located 10 ft upgradient to the west, and P3 is located 5 ft crossgradient of the treatment well to the north.

6.4 Flow Sensors

A total of five flow sensors were emplaced in three boreholes (F1, F2, and F3; see Figure 6.1). The flow sensors were designed to give both the magnitude and direction of groundwater flow in three dimensions. For the flow sensors to provide a representative measurement, they must be surrounded by the aquifer matrix. To accomplish this, small-diameter boreholes (3 to 4 in.) were drilled, the flow sensors were emplaced, and the boreholes were then allowed to collapse back in around the sensors so that they would be encased in the natural sediments. Flow sensors in boreholes F2 and F3 were stacked on a single casing string: the top flow sensor was positioned vertically at ~32.5 ft and the lower flow sensor at 47.5 ft below ground surface, or approximately in the middle of the screened intervals in the monitoring wells. Borehole F1 had a single flow sensor placed at a depth of ~47.5 ft.

Boreholes F1, F2, and F3 were located at radial distances of 50, 34.5, and 17.5 ft, respectively, from the demonstration well. Boreholes F1 and F2 were positioned due south of the demonstration well, while the closest, F3, was located southwest of the demonstration well. Borehole F3 was placed slightly upgradient of the demonstration well because the original location directly crossgradient was drilled with an air-rotary rig, and the borehole would not adequately collapse back around the sensor.

A replacement borehole was drilled slightly upgradient of the demonstration well using an auger rig. Borehole F1 was drilled with a sonic rig, and an auger rig was used to drill F2.

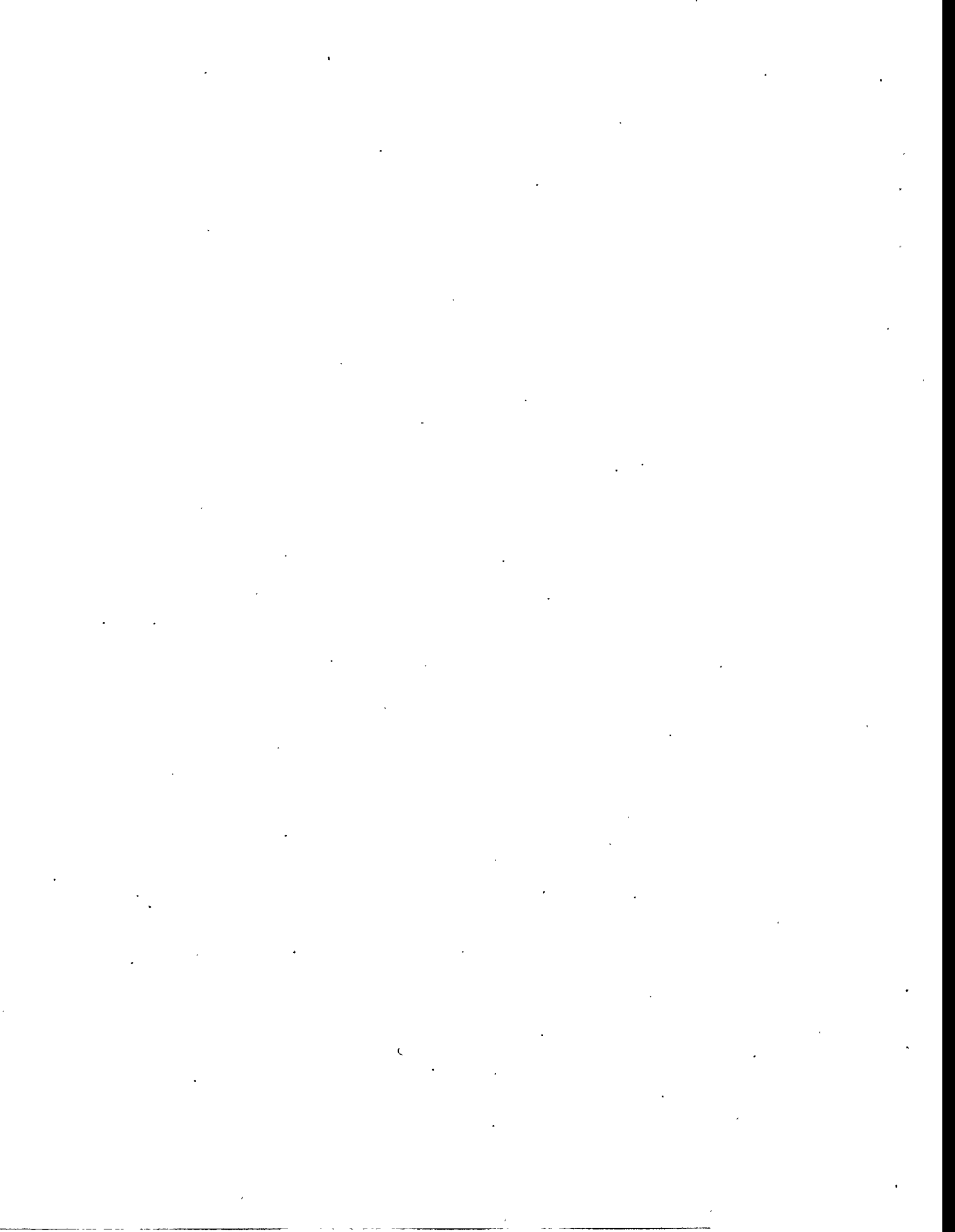
The upper flow sensors in boreholes F2 and F3 failed and no measurements were available. It is believed that the sensors leaked as a result of a poor epoxy seal. This problem was remedied for future flow sensors. The 3 lower sensors in F1, F2, and F3 all provided data (given in Section 11.7).

6.5 Characterization Wells

Wells C1 and C2 were drilled for site characterization and were used to determine if the site could support the in-well vapor-stripping demonstration. The wells were continuously cored to the "point of refusal," which was the competent bedrock below the site at ~55 ft below ground surface. The core was used for geologic descriptions and physical testing and analysis. Each well was completed with 2 screened intervals in a single 4-in.-dia. casing string. The top screen was located at 30 to 35 ft below ground surface, and the lower screen at 45 to 50 ft below ground surface.

6.6 CERCLA Monitoring Wells

The CERCLA monitoring wells (19-MW03 and 19-MW04; see Figure 6.1) were constructed as part of the remedial investigation at Site 19 prior to the demonstration. Both wells were constructed of 4-in.-dia. polyvinyl chloride casing, with stainless steel screens. Well 19-MW03 has a screened interval between 19.5 and 39.5 ft, and well 19-MW04 is screened between 60 and 70 ft in the bedrock.



7.0 Site Characteristics

Site-specific information was obtained from wells drilled for the demonstration. Information from these wells was used to characterize the site to interpret the data collected during the demonstration and to develop the conceptual model for the computer simulations.

The characterization activities included the determination of the site's stratigraphy, hydrology, soil chemistry, water chemistry, and contaminant(s) of concern. The site characteristics are summarized in Table 7.1.

Table 7.1. Summary of Site Characteristics

Parameter	Value
Groundwater contaminant	Trichloroethylene
Depth to water	25 ft
Aquifer thickness	25 ft
Aquifer sediment	Fine sands with interbedded silts
Particle density	2.612 to 2.637
Bulk density	1.81 to 2.2
Porosity	0.155 to 0.313
Vertical hydraulic conductivity	1 ft/d
Horizontal hydraulic conductivity	10 ft/d
Anisotropy ratio	0.1
Horizontal hydraulic gradient	0.005
Vertical hydraulic gradient	0.1 upward
Average linear velocity	0.2 ft/d

7.1 Stratigraphy

The site was previously investigated (Engineering Science 1988, 1989) and a draft remedial investigation report was completed on Site 19 (Earth Technology 1994).

The stratigraphy of the site consists of unconsolidated sediments overlying granitic bedrock. The sediments are alluvial and lacustrine deposits of sands with some gravels and smaller fractions of caliche, silt, and clay. The thickness of the alluvium is ~50 ft near the demonstration site. Weathered bedrock and clay are encountered at ~50 ft, below which is highly fractured bedrock. Two clay/caliche

layers were identified in the characterization wells at 29 and 44 ft below ground surface, each ~0.5 ft thick. The sediments are highly variable in the area, and correlation of sedimentary layers between wells C1, C2, and D1, which are 50 ft apart, could not be completed with a high degree of certainty. The silt-clay/caliche layer at 44 ft was continuous between the wells but was not present at 29 ft in well C1 (Figure 7.1). There was a significant amount of calcium carbonate in some of the samples, ranging from <0.2% to 17.2% at a depth of 50 ft (the contact with weathered bedrock). The zones with high percentages of calcium carbonate are thought to be paleosols and/or caliches.

A stratigraphic column was generated for the demonstration site from core samples obtained from wells C1, C2, and D1 and from geophysical logs from monitoring wells M1, M2, M3, M4, and M5. Core samples from the characterization wells were analyzed in the laboratory to determine porosity, grain density, grain-size distribution, liquid permeability, and gas permeability.

7.2 Groundwater

Groundwater beneath the demonstration site occurs as an unconfined to semiconfined aquifer in the alluvium at ~25 ft below ground surface. At the base of the alluvium is a weathered bedrock and clay layer at ~50 ft below ground surface that is believed to form a semiconfining layer above the fractured bedrock aquifer. The horizontal gradient at Site 19 is ~0.005, and there is a consistent downward vertical gradient within the alluvium (Earth Technology 1994). Aquifer tests were conducted at Site 19 in an area ~800 ft away from the demonstration site. The test results indicated that the hydraulic conductivity in the alluvium ranges from 120 to 740 ft/d. Aquifer tests conducted on wells in the fractured bedrock indicated a range of hydraulic conductivity of between 0.0023 and 8.78 ft/d (Earth Technology 1994). Additional aquifer tests were conducted to determine the specific characteristics of the demonstration site, including slug testing, constant-rate discharge testing, and dipole testing. An estimate of the horizontal hydraulic conductivity at the demonstration site is between 4 to 10 ft/d. Test data also indicate an apparent hydraulic connection between the alluvial and bedrock aquifers. The vertical hydraulic conductivity at the site was planned to be determined using the dipole flow-testing method; however, the late-time drawdown curve was not distinct enough for an accurate interpretation using the Kabala (1993) method. Dipole testing, however, provided some information on the variability of the conductivities between the upper and lower screened intervals and some information on what water-injection rates the formation could maintain.

7.3 Surfacewater

There is a surfacewater pond located ~400 ft south of the site. This pond is a catchment for storm runoff and some waste waters. Base personnel believe that the pond is clay lined and, based on potentiometric maps (Earth Technology 1994), the pond does not appear to have a significant effect on the water table in the area. Water-level data collected over several years by Earth Technology (1994) indicate that the primary source of recharge to the aquifer is from rainfall infiltrating through the alluvium. In 1992, there was unusually high rainfall (> 12 in. for the year), with most of the rain concentrated in

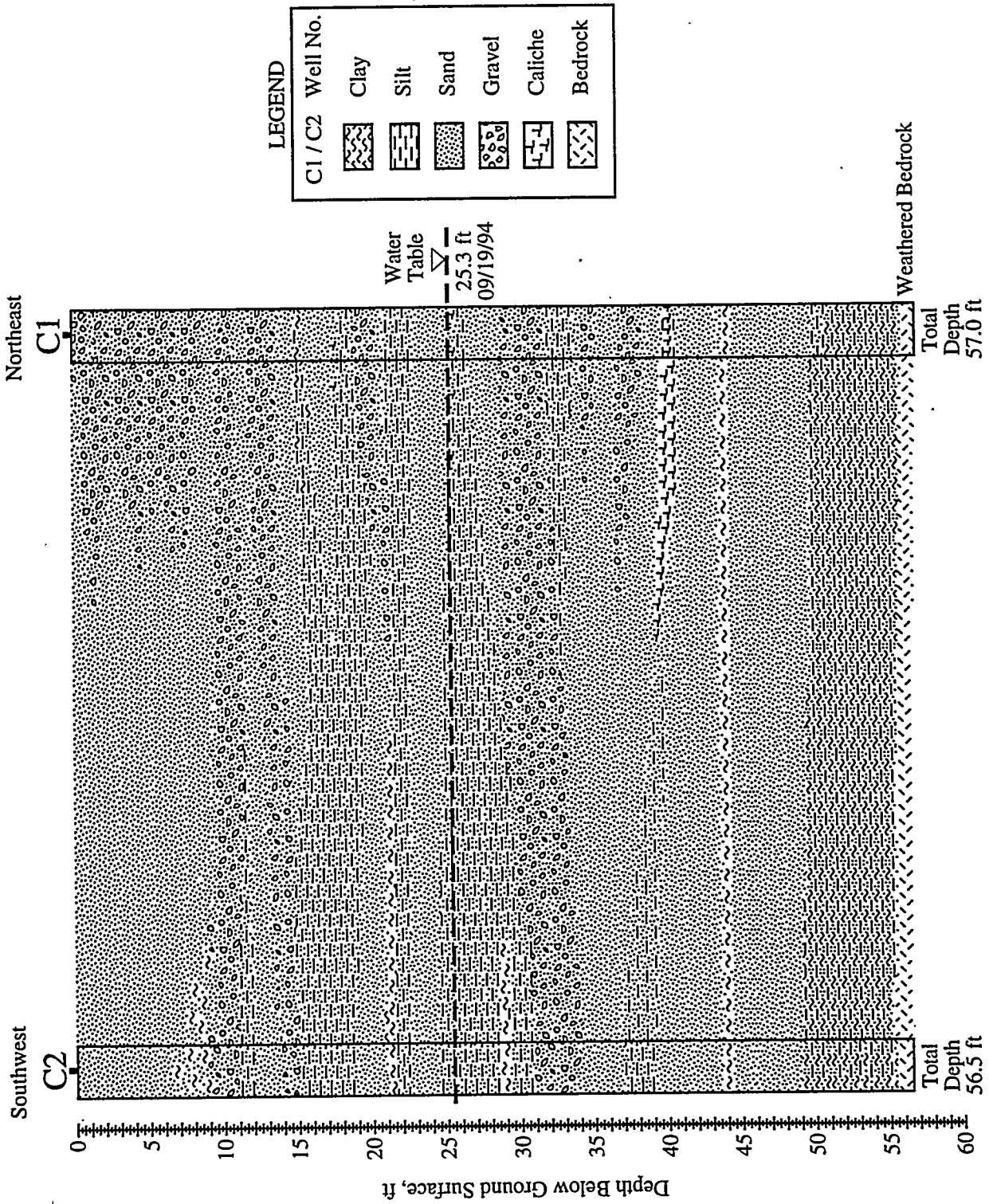


Figure 7.1. Geologic Cross Section of Demonstration Site

January through March (7.66 in.). Recharge from this period of rainfall peaked 2 to 3 months after the precipitation in the alluvium (Earth Technology 1994). The peak in the bedrock aquifer was delayed to late in 1993.

7.4 Soil Chemistry

The depositional environment of the sediments in the area is alluvial/lacustrine. The surface sediments are essentially a dry lakebed. These conditions produce high calcium carbonate accumulations and appreciable quantities of neutral soluble salts in the soil. These soil conditions are common in Southern California desert environments and can be a concern in terms of the infiltration capacities of the soil. When relatively low-ionic-strength waters come in contact with sodic soils, sodium is displaced, causing clay colloids to disperse and some clays to swell. This results in the clogging of the pore spaces and a decrease in permeability, a condition called clay dispersion (Brady 1974). Figure 7.2 shows the relationship to the sodium percentage and total dissolved solids in the porewater. The sediments taken from various depths are plotted in relation to three zones, corresponding to dispersive, intermediate, and nondispersive (Serard et al. 1976). The dispersive nature of the sediments generally decreases with depth.

7.5 Water Chemistry

The water-quality type in the alluvium at Site 19 is highly variable, with total dissolved solids concentrations ranging from 286 to 55,800 mg/L (Earth Technology 1994). The water-quality type in the shallow alluvium was classified as sodium chloride grading to sodium calcium chloride in the deeper portions of the aquifer (Earth Technology 1994). Near the demonstration site, the sodium adsorption ratios of the water decrease with depth, with values in the upper aquifer ranging from 15 to 17 and from the bottom of the alluvial aquifer ranging from 6.5 to 7.

The water at the site had high concentrations of calcium (67 to 160 mg/L), with the highest calcium concentrations in the lower zones. These conditions could contribute to precipitation of the calcium (scaling) in the demonstration if not compensated for. The aquifer also has high dissolved oxygen (5 to 8 mg/L). Initially, dissolved oxygen was considered as a tracer, but the background concentrations were too high to discern changes resulting from operation of the vapor-stripping well.

7.6 Contaminant of Concern

Previous investigations at Site 19 have identified TCE in groundwater occurring at a maximum concentration of 6800 $\mu\text{g/L}$ at the source area (Earth Technology 1994) ~800 ft hydraulically upgradient of the demonstration site. The maximum concentration of TCE measured at the demonstration site was 502 $\mu\text{g/L}$, but generally averaged 300 $\mu\text{g/L}$. The highest concentrations of TCE occur near the base of the alluvium. Other contaminants identified in the groundwater within Site 19 are petroleum hydrocarbons and related aromatic VOCs and naphthalene. Only TCE and its degradation product, 1,2-cis-dichloroethylene, were detected in the groundwater at the demonstration site. No additional

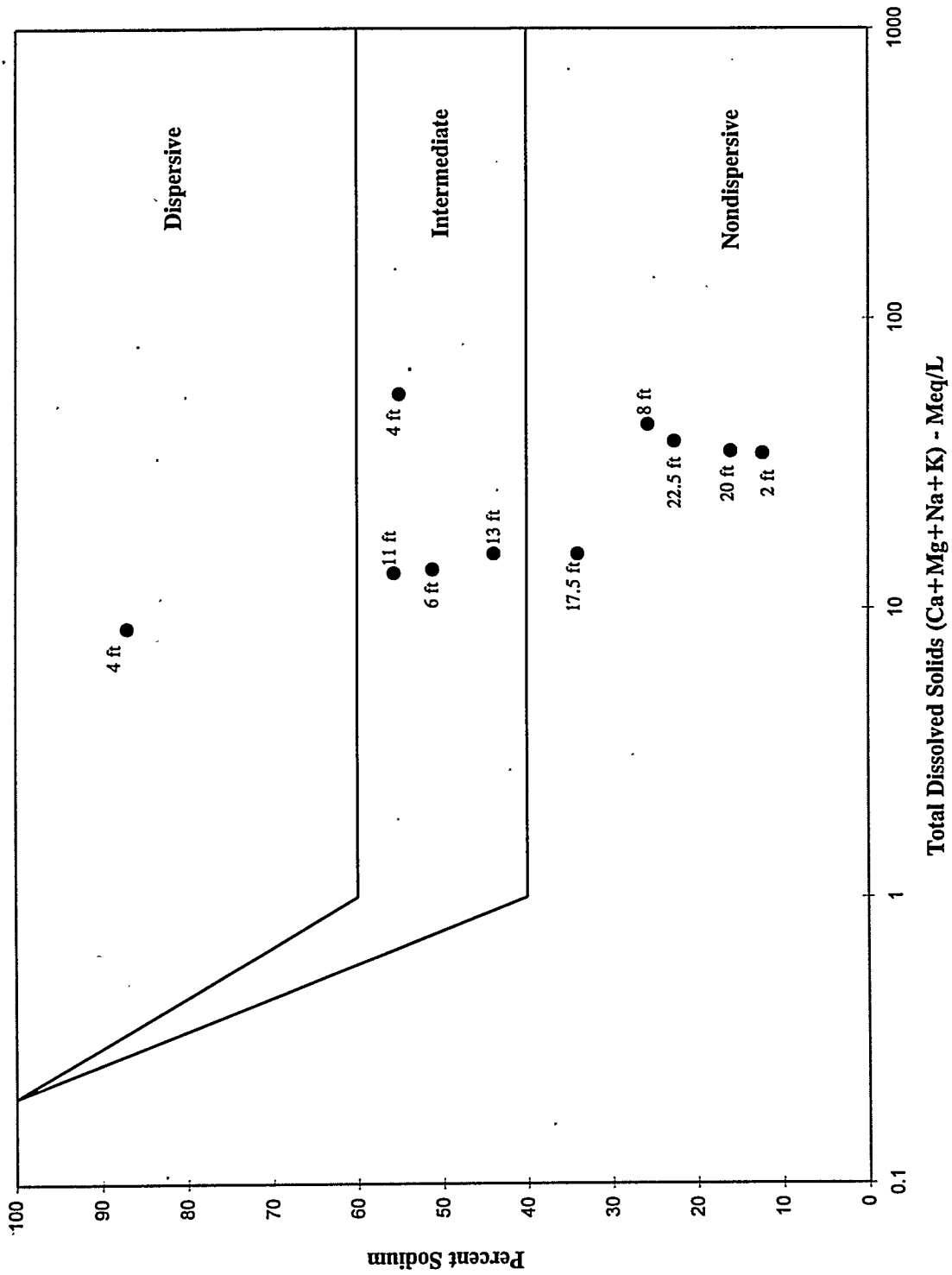


Figure 7.2. Dispersive Clay Zonations

contaminants of concern were identified in the soil or groundwater at the demonstration site following a comprehensive sampling effort that included analyses for volatile and semivolatile organics; metals; gross alpha, beta, and gamma; polychlorinated biphenyls, and pesticides.

8.0 Methods

Many measurements are essential in any groundwater remediation project. Those that are specifically important to the in-well vapor-stripping system demonstration at Edwards AFB are the following: measuring water-flow (pumping) rate, real-time off-gas readings, three-dimensional velocity measurements around the pumping well, and groundwater and soil chemistry. The methods for attaining these parameters follow.

8.1 Water-Flow (Pumping) Rate

An important parameter to measure during the operation of the system is the water-flow rates, or pumping rates, that are induced by air injection. Because water is not withdrawn from the well casing, a means to measure the water flow within the casing was needed. The standard method for measuring water-flow rate is the use of an in-line flow meter (turbine or other type) but this could not be done because of the large-diameter casing, multiphase turbulent flow of the air-water mixture, and submergence of the meter.

Several techniques were tested, each with varying success: a downhole weir, orifice plate, empirical flow curves derived in the laboratory testing, and recharge tests of the demonstration well.

8.1.1 Downhole Weir

A downhole weir was designed to measure the flow of water as it exits the eductor pipe into the annulus where it reinfilters (Figure 8.1). A standard weir measures flow in an open channel, where water is directed over a "v" notch of known dimensions. The height of water behind the "v" notch is related to the water-flow rate in the channel. An adaptation of this concept was developed in the form of a downhole weir. The in-well application of this weir captures vertical flow of water in the well casing and channels it across the "v" notch. The height of the water in the weir can be remotely monitored using a pressure transducer (Gilmore and Francois 1996).

The weir was constructed and calibrated during the laboratory testing of the system. The weir was designed to measure flow rates between 10 and 40 gpm, which turned out to be above the flow range of the field demonstration (2 to 10 gpm). As a result, the weir did not have sufficient resolution for this application; however, it did have some additional benefits that included a convenient location to sample water exiting the eductor pipe and allowed more time for the water to de-gas before reinfiltrating into the sediments.

8.1.2 Orifice Plate

An orifice plate built by EG&G was installed in the eductor pipe and was used to provide another method for measuring the water-flow rate. The orifice consisted of a thin acrylic plate with a 1.5-in.

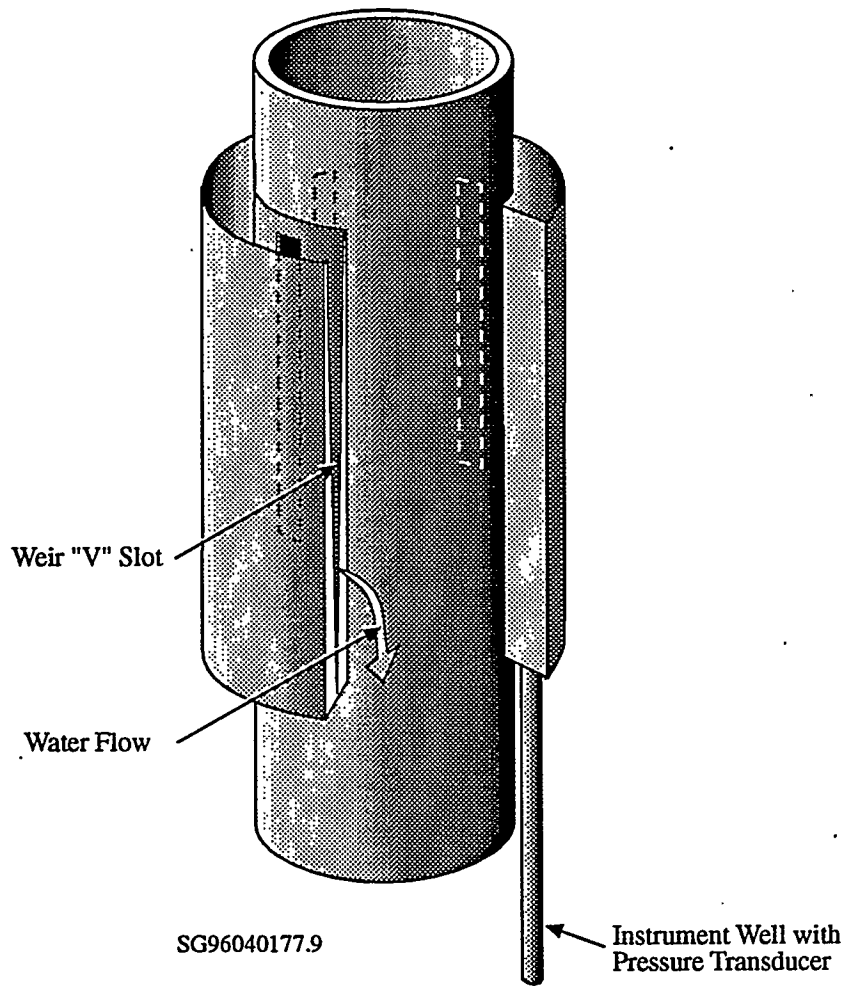


Figure 8.1. Down-Well Water-Flow Meter (Weir)

hole, or orifice. The orifice plate was placed on the eductor pipe below the air-injection point, and all the water entering the eductor pipe was channeled through the orifice. By measuring the pressure differential across the orifice, a water-flow rate could be determined.

The differential pressure measurements fluctuated rapidly as a result of the variable flow within the eductor pipe. From the laboratory testing, it was observed that airlift pumping does not produce an even flow rate but lifts water in surges and that there are many embedded cycles of bubble sizes and flow that need to be compensated for. The measurements should be collected using a data logger, with the sampling rate frequent enough to not be biased by the cycles. The data could also be smoothed to filter some of the noisiness caused by the turbulent flow.

8.1.3 Empirical Operating Curves

An alternate method to determine the water-flow rate in the system is to use a set of empirical operating curves. These curves were developed during laboratory testing of a full-scale model of the in-well vapor-stripping system. Water-flow rate in the laboratory was measured by channeling the airlifted water into a pipe to be measured with a calibrated paddle-wheel-type flow meter. These curves can be used to determine the water-flow rates based on total lift and inlet airflow volume. The lift and inlet airflow volume can each be determined in the field relatively easily and, therefore, these operating curves could be used in lieu of downhole flow meters. The operating curves shown in Figure 8.2 include total lifts that range between 20 and 35 ft in 5-ft increments. A physically based airlift pumping model was also developed from the laboratory data and can be used to calculate flow rates (Francois et al. 1996). The difficulty in using the curves was that at the low-flow rates at which the system was operating, the curves did not provide the resolution (± 0.5 gpm) needed.

8.1.4 Recharge Rate

Perhaps the most representative and accurate measurement of flow for the system was determined by measuring the recharge rate of the upper zone in the demonstration well. The "return height" in the upper zone remained steady during operation of the system at ~18 ft from the bottom of the upper screened zone. The flow of water required to maintain this height was measured directly with a water-supply hose and a measuring bucket. These measurements should be reasonably representative of the infiltration rates when the system is operating. During operation, however, there is a larger downward gradient imposed on the system by extracting water from the lower screen, so these estimates will be more conservative.

8.2 Off-Gas Readings

Off-gas concentrations of TCE and carbon dioxide were measured using an infrared photoacoustic spectrometer manufactured by Brüel and Kjaer, Naerum, Denmark. This spectrometer takes advantage of the unique spectral properties of the VOCs to identify the types and quantities in a gas stream. A volume of gas (~150 mL) is drawn through an analysis chamber that contains sensitive acoustic microphones. The gas is then irradiated with a pulsed, midinfrared band of light selected by a narrow bandpass filter. The choice of filter is determined by the principal absorption band of the target gases, in this case TCE and carbon dioxide. The instrument can be equipped with up to five filters for simultaneous determination of separate analytes. A sixth channel is used for correction of water interferences. For this setup, one filter was selected for TCE, a second for carbon dioxide, and a third to correct for water vapor. The analyte gas absorbs light to a degree dependent on the concentration of the contaminant in the gas. The absorbed radiation is then primarily converted to heat. The change in temperature produces a pressure wave that is sensed by the microphones. Analyte concentration is measured as a function of acoustic wave amplitude. Lower detection limits for most analytes tend to be in the low, or sub-part-per-million, range. The instrument was calibrated across a range from 0 to 620 ppm for TCE.

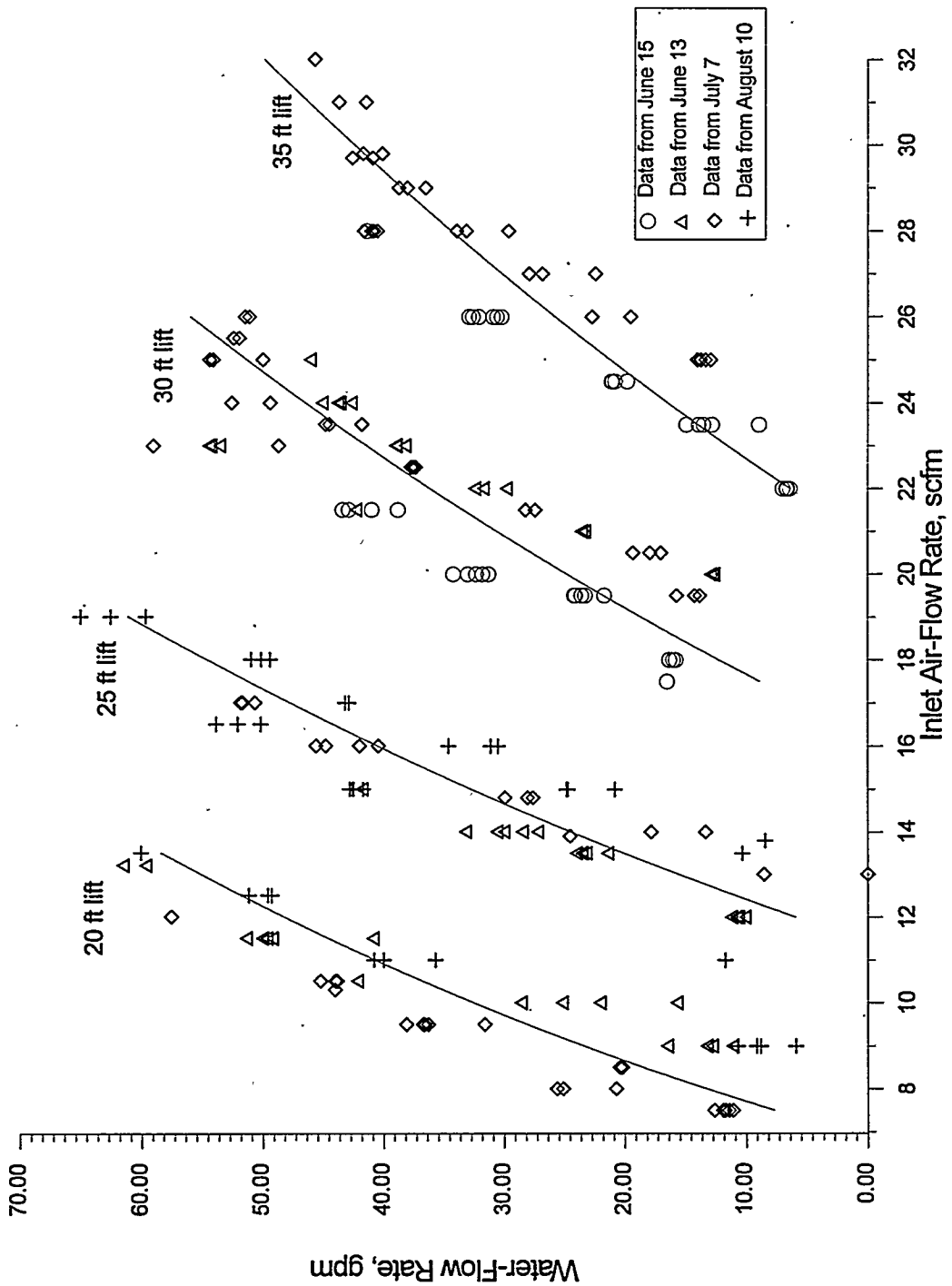


Figure 8.2. Operating Curves Using a 400-Micron Sparger Element

8.3 Groundwater Velocity Measurements

To help define the system's zone of influence, a suite of in situ permeable flow sensors were installed. These sensors use a thermal perturbation technique to directly measure the direction and magnitude of the full three-dimensional groundwater flow-velocity vector in unconsolidated, saturated, porous media (Ballard 1996). The instrument is a device that essentially heats the groundwater as it flows across the probe. Relatively cool temperatures are observed on the upstream side; warmer temperatures on the downstream side. The temperature distribution around the probe is a function of the direction and magnitude of the groundwater-flow velocity past the cylinder. Three flow sensors were installed (see Figure 6.1). The flow-sensor technology was licensed to Hydro Technics, Inc., Albuquerque, New Mexico, for commercialization.

8.4 Groundwater Parameters

Dissolved oxygen, pH, and temperature of the groundwater were manually recorded daily when an operator was at the site, using the H2OG Hydroprobe™. Water-level measurements in the demonstration and monitoring wells were collected using pressure transducers with a data logger and manually using an electric water-level tape.

8.5 Groundwater Sampling

Comprehensive baseline groundwater sampling and trend analyses for VOCs were conducted. The baseline sampling for a comprehensive list of contaminants (metals, volatile organics, semivolatiles, lead, pesticides, polychlorinated biphenyls, gross alpha, gross beta, gross gamma, alkalinity, anions, pH, and temperature) was analyzed by a U.S. Environmental Protection Agency-approved laboratory, Data Chem, Salt Lake City, Utah. The trend analyses of the VOCs in the groundwater were determined using gas chromatography by Pacific Northwest National Laboratory and Stanford University. Groundwater sampling for volatile organics was accomplished by using a bailer. Approximately one borehole/filter pack volume was evacuated with the bailer prior to collecting a sample. The samples were collected in 40-mL amber vials and preserved with ice.

8.6 Lithologic Sampling

Continuous core was collected from the drilling of wells C1, C2, and D1. The lithologic descriptions were made from examination of the core. The core was then cross-referenced with the geophysical logs of the monitoring wells.

Sediment samples for chemical analysis were collected every 5 ft, beginning at ground surface and continuing until the final depth of the borehole. Analyses completed on the samples were metals, volatiles, semivolatiles, pesticides, polychlorinated biphenyls, lead, and total organic carbon. Samples were analyzed by Data Chem and Pacific Northwest National Laboratory.

Sediment samples for unsaturated flow analysis were collected every 10 ft from ground surface to the static water level to measure hydraulic conductivities under varying moisture content. The Washington State University-Tri-Cities laboratory conducted the analysis using the unsaturated flow apparatus, which employs a centrifuge for measuring air and fluid movement in porous media. The centrifuge speeds the analysis time over typical gravity-dependent laboratory measurements.

Sediment samples for physical properties were collected every 5 ft and analyzed for grain-size distribution, moisture, bulk density, and calcium carbonate at the Pacific Northwest National Laboratory.

9.0 Design of Aboveground Apparatus

The apparatus used to control the in-well vapor-stripping system operation for this demonstration includes a treatment trailer that contains all the hardware and software described in the following sections.

9.1 Treatment Trailer

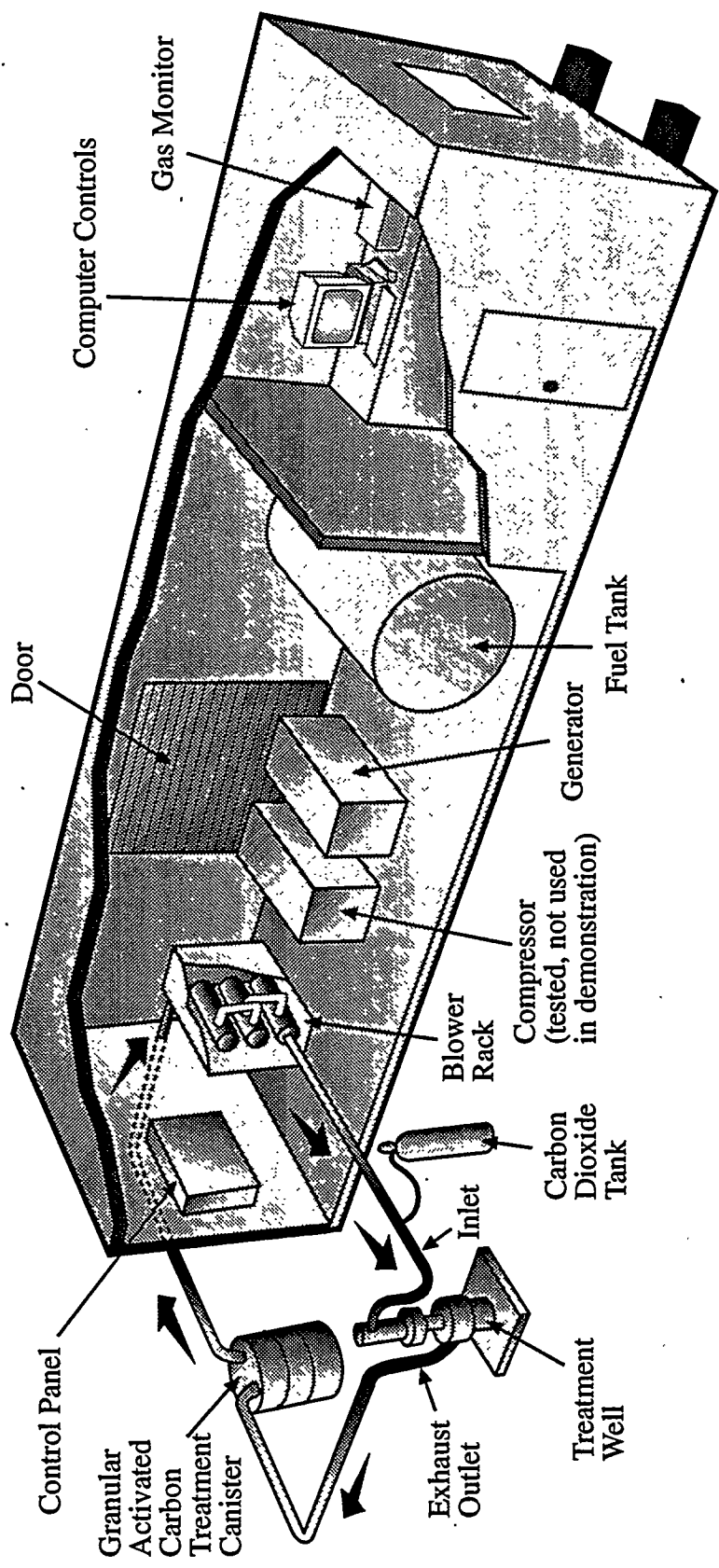
The treatment trailer is a steel cargo container converted to include roll-up doors, equipment, and an office. This skid-mounted trailer can be moved from site to site on the back of a semitruck and trailer (Figure 9.1).

The equipment in the treatment trailer includes an air compressor, blowers, generator, instrumentation to control the system, fuel tank, and high-efficiency particulate-air (HEPA) filter. Although the system was designed to be a stand-alone, self-contained unit, there are connections on the trailer for external line power. Part way through the demonstration, an external power line was connected to the trailer and the generator was taken off line. There are also external hookups for the off-gas treatment, so that the treatment selection is flexible. For this demonstration, a granular, activated carbon treatment canister was used to filter the off-gas. The HEPA filter was included in the design because the trailer was originally designed for operation at the U.S. Department of Energy's Hanford Site where the off-gas could potentially contain radioactive particulates. The HEPA filter was bypassed during the Edwards AFB demonstration. There are enough system controls and plumbing in the trailer to operate up to three wells simultaneously.

The air compressor is a diesel, Lindsay 80-K™. The compressor uses a Kubota 1702-B water-cooled engine; its rated capacity is 74 cfm at 100 psi. The air blowers used were Rotron™ rotary vane blowers (PRP230AW72) capable of producing airflow rates of 20 cfm at 15 psi. The generator is a 25-kVA Multiquip WhisperWatt™ AC Model DCA-25SSAI. The generator uses an Isuzu QD-60 water-cooled engine, with a rated capacity of 26.5 kVA (21.2 kW), 3-phase, 120/240 V. A double-walled, 1000-gal fuel tank is included in the trailer, and the trailer can operate for ~15 days between refueling if used with no external power.

9.2 System Control and Data Logging

The treatment trailer monitors the system's functions on a computer screen using Labview™ software. All the system's functions are recorded automatically into a data file in the computer. The computer screen is interactive and allows the operator to control the treatment processes. Figure 9.2 is a printout of the interactive screen. The main categories that are monitored on the screen are the compressed air supply, well-head exhaust, well instrumentation, water-flow rate, process conditions, generator condition, and compressor condition. There are several functions under each of these



SG96080282.4

Figure 9.1. Treatment Trailer

categories that are monitored and recorded into a data file at a rate specified by the user. In general, the data-collection rate is in the range between 1 and 10 min.

Under the "Compressed Air Supply" category, the following functions are monitored and recorded: air pressure (psig), airflow (cfm), and temperature (deg F). The airflow set rate on the compressor can be adjusted on the screen and is recorded in the data files.

Under the "Well-Head Exhaust" category, the airflow rate (cfm), temperature (deg F), and pressure (psig) are displayed and recorded.

The water-flow rate (gpm) is calculated from the downhole weir in the well and is displayed on the screen and recorded in the data files.

The control screen also allows the entry of comments and several well parameters from the demonstration well and the surrounding monitoring wells. Under manual data entry, all monitoring wells are listed with the following categories: dissolved oxygen, temperature, pH, and water level. Measurements of dissolved oxygen, temperature, and pH are taken manually using the H2OG Hydroprobe™. For water levels, an electrical sounding probe or steel tape is used. The results are entered into a designated area on the control screen and time stamped and recorded in the data file.

For the "Generator Condition" and "Compressor Condition" categories, oil and water temperature fault lights (to indicate service attention), and hours on are displayed on the control screen and recorded in the data file.

Under the "Process Conditions" category, the following functions are displayed on the control screen and entered into the data files automatically: temperature in process end of trailer (deg F), fuel level (gal), process heat exit temperature (deg F), VOC concentration (ppmV), VOC cumulative concentration (mg), rear process differential pressure (psi), HEPA differential pressure (psi), carbon bed differential pressure (psi), carbon bed outlet temperature (deg F), compressor inlet pressure (psi), compressed air supply pressure (psi), compressed air supply temperature (deg F), and fuel consumption (gal).

10.0 System Optimization and Refinements (Lessons Learned)

During the course of testing the in-well vapor-stripping system at Edwards AFB, it was found that the system could be optimized in several crucial ways: substituting the air compressor with blowers, controlling organic and inorganic precipitation, adequately developing the pumping and infiltration zones and maintaining reinfiltration capabilities of the demonstration well, using an eductor pipe to increase pumping capacity, using a closed-loop system, and correcting for condensation effects to minimize maintenance.

10.1 Blowers Versus Air Compressor

Initial testing of the system began in August 1995 and lasted for 3 days (Figure 10.1). The system was stopped because oil from the compressor was being blown by the oil dropout filter in the air line and a small amount was detected in the well. The oil blowby was caused, in part, by the high summer temperatures in the desert environment ($> 100^{\circ}\text{F}$), which caused the air-compressor engine to run hot and vaporize some of the oil. A series of oil filters were installed in the air line to minimize the oil problems; however, this also increased maintenance of the system. To reduce maintenance and eliminate potential oil contamination, the air compressor was replaced with blowers. The air blowers used were Rotron™ rotary vane blowers capable of producing airflow rates up to 20 cfm at 15 psi. Use of the blowers also reduced the high maintenance requirements of the diesel engine. The blower manufacturer's maintenance guidelines indicate the only planned maintenance/service activity is bearing replacement every 15,000 to 30,000 hours of operation (every 1.5 to 3 years).

Blowers may be used in applications where the pressure requirements of the system are < 15 psi (30- to 35-ft submergence depths, assuming minimal friction losses in the pipes). The air compressor may still have applications that require higher system pressures.

The blower operation was very efficient, with only minor shutdowns as a result of overloading. The overloading of the blowers resulted in part by running the system in a closed loop (Section 10.5). The system was protected from overloading by adding a pressure-release valve, and the pressure buildup in the system was reduced by using larger-diameter pipes (2 in. or greater) to minimize friction losses and by raising the depth of the air-injection point in the water. The pressure in the air-injection lines was eventually maintained at ~ 7 psi, 50% of the pressure capability of the blowers. One blower failed and was required to be replaced after ~ 3 months of operation. The blowers were operated at higher-than-specified pressures for a period of time, which may have contributed to their failure.

10.2 Controlling System pH

The groundwater at the demonstration site is nearly saturated with respect to calcium. When water is aerated, carbon dioxide is stripped out of the water, raising the pH. At higher pH, some minerals,

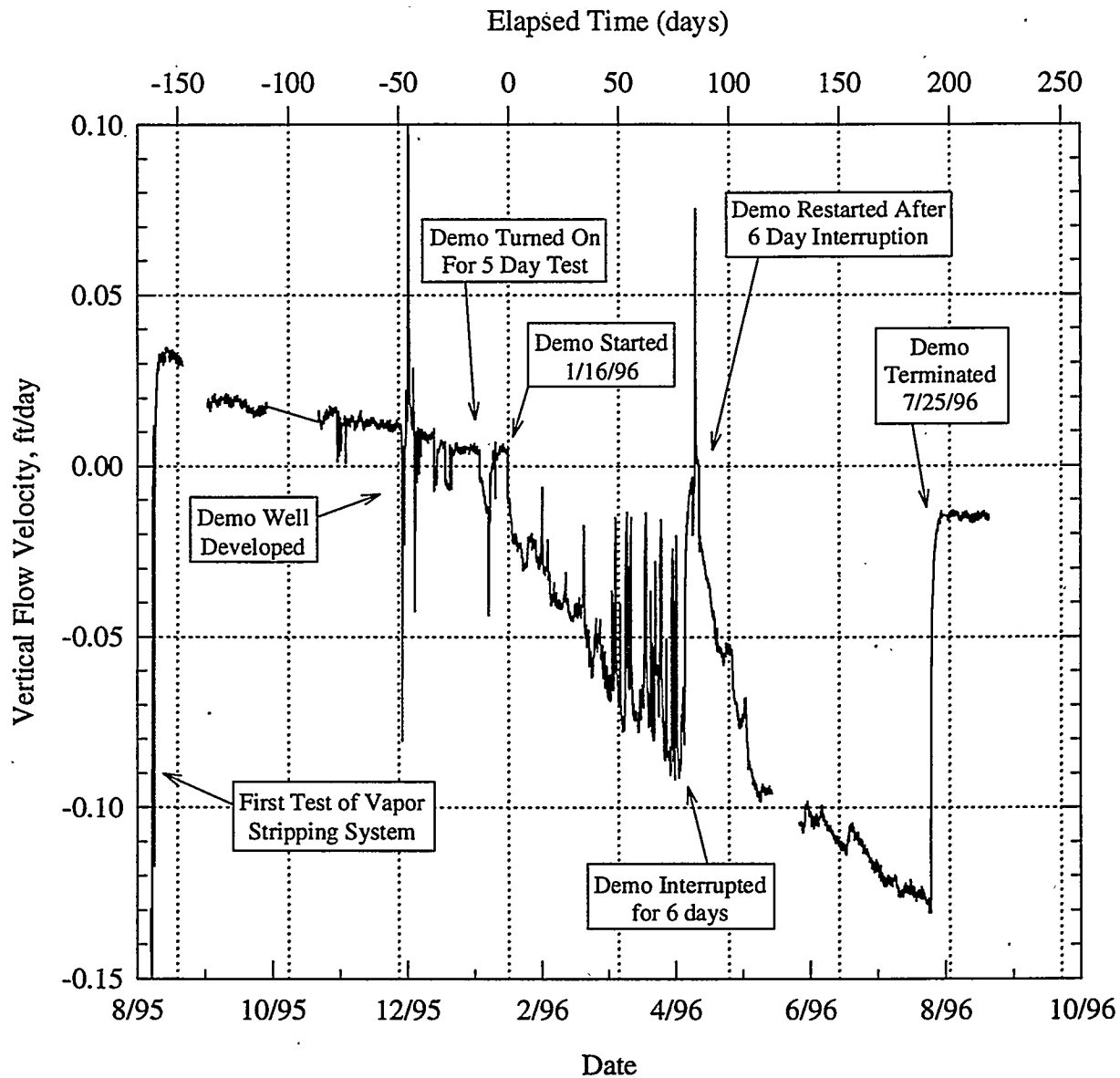


Figure 10.1. System Operation Reflected by Flow-Sensor Data at F3 (Days of operation are shown most effectively by the data from flow sensor F3. When the system was not operating, the flow would return to zero. Section 11.7 gives more detail on flow-sensor results.)

such as calcite, will precipitate out and coat the well screens (scaling), which causes an associated reduction in permeability in the reinfiltration zone. To minimize the amount of calcite precipitation from aerating the water, the pH of the system was controlled by adding carbon dioxide into the air stream injected in the well. The added carbon dioxide replaced the carbon dioxide removed from the system through aeration and maintained the pH. The target pH level was 0.2 to 0.4 below the background pH of 7.45. This provided a safety factor by decreasing the possibility of plugging the

treatment well. To maintain the pH at 7.2, carbon dioxide was added at a rate approximately equal to 0.2% of the total airflow rate. At an inlet airflow rate of ~65 cfm, carbon dioxide was added to the air stream at a rate of 0.15 cfm (9 cfh on the flow meter). The concentration of carbon dioxide in the air stream was measured by the Brüel and Kjaer vapor meter and averaged 38,000 ppm.

Because this is a closed-loop system, in which the exhaust air is treated and reinjected into the well, the consumption of carbon dioxide was minimized. It is likely that a higher injection rate of carbon dioxide is required in an open-loop configuration, where the exhaust air is released to the atmosphere.

Initially, the carbon dioxide-injection line was run directly into the air-injection line, but because of the surging airflow in the line, the backpressure on the injection line was constantly changing and affecting the carbon dioxide-flow rate. To compensate for this and protect the pressure regulator, a backflow preventer was placed in the carbon dioxide line. A welder's flow meter was used to control and monitor the flow rate from the carbon dioxide tank.

10.3 Infiltration/Reinfiltration

The rate-limiting step for the system was the reinfiltration rate of the upper zone in the well. The aquifer could initially produce more water than the vadose zone could accept. In addition, the infiltration rate decreased following the initial system tests. The low infiltration rates are believed to have resulted from both plugging by fine-grained sediments produced during the initial pumping and the effects of dispersive clays resulting from low-ionic-strength waters coming in contact with vadose zone sodic soils. To regain the infiltration capacity, both the upper and lower zones in the demonstration well were redeveloped through a combination of physical and chemical treatment.

Airlift pumping creates a surging action that will pull in fine-grained sediments from around the well. Because typical applications of the technology include continuous operation for extended periods of time, it is imperative that the well be fully developed before starting the system or all the fines from the lower zone will be pumped into the infiltration zone and plug up the well. Development of treatment wells must be more extensive than what is now typical for developing monitoring wells (i.e., overpump until the turbidity is low and the groundwater parameters are stable). Prior to use as a treatment well, the well must be repeatedly surged and overpumped until clean.

It is equally important to develop the upper zone to maximize the infiltration rates. In some locations, this may entail both physical and chemical treatment.

The water pumped into the infiltration zone may not be in equilibrium with the soil chemistry. This is particularly true in the desert southwest, where the soils are often sodic (high in sodium) and the aquifer waters relatively low in sodium. When low-ionic-strength waters come in contact with sodic soils, sodium is displaced from the soil that, in turn, can both displace clay colloids and cause deflocculation, or swelling, of the clays and result in clogging of the pore spaces (Brady 1974). Samples collected during well construction indicated the sodium percent in the soils was high, particularly in the zones near the surface, and the water from the pumping zone near the bottom of the aquifer had

relative low-ionic strength. To control these "dispersive" clays, calcium can be added to the water in the form of gypsum or calcium chloride. The calcium will substitute for the sodium on the clay and minimize flocculation and dispersal of the clays. In California, the agricultural community uses these methods to increase water penetration from irrigation (Oster et al. 1992).

To develop the upper zone (reinfiltration zone of the demonstration well), the well was filled with potable water from the base water supply and then surged using a surge block operated by a pump-setting rig. The surging action pulled fine sediments into the well, where they were evacuated using a submersible pump. The zone was physically surged like this for two days. On the third day, calcium chloride was then added to the water at a concentration of ~0.02% and surging of the well continued for three additional days. There was a substantial improvement in the infiltration rate of the upper zone following development, and the majority of the improvement occurred after the calcium chloride was added to the well.

After development and continuing during the operation of the system, calcium chloride was periodically added to the recharge waters at a rate of ~0.7 kg/wk to maintain the infiltration rate. Over the 6-month operation of the system, the infiltration rates of the demonstration well actually increased. The infiltration rate of the demonstration well in January was 2.5 gpm and in April it was 10 gpm. This increase in infiltration rate is believed to be the result of changes in the vadose zone around the well. One explanation is that the calcium chloride added to the system stabilized the fines around the infiltration zone, resulting in a higher hydraulic conductivity. Some increase is also likely from increasing the saturation of the sediments around the well, which would increase the relative hydraulic conductivity, but the increase in infiltration rate was gradual over the course of the demonstration and the saturation of the sediments would have been more rapid.

10.4 Use of Eductor Pipe to Optimize Pumping Rates

During testing of the system, air was observed in samples collected from well D2a, which is completed in the filter pack of well D2. With the air-injection point at the bottom of the well screen, air was entering the filter pack. To correct this, a sleeve was placed over the screen to keep the air from exiting the well. This sleeve was in the form of a 4-in.-dia. polyvinyl chloride eductor pipe (see Figure 6.3[c]). The eductor pipe extended from just above ground surface to the bottom of the well. Water entered the eductor pipe through holes cut in the side of the pipe very near the bottom. This allowed the air-injection point to be lowered in the well without permitting the air to escape to the filter pack.

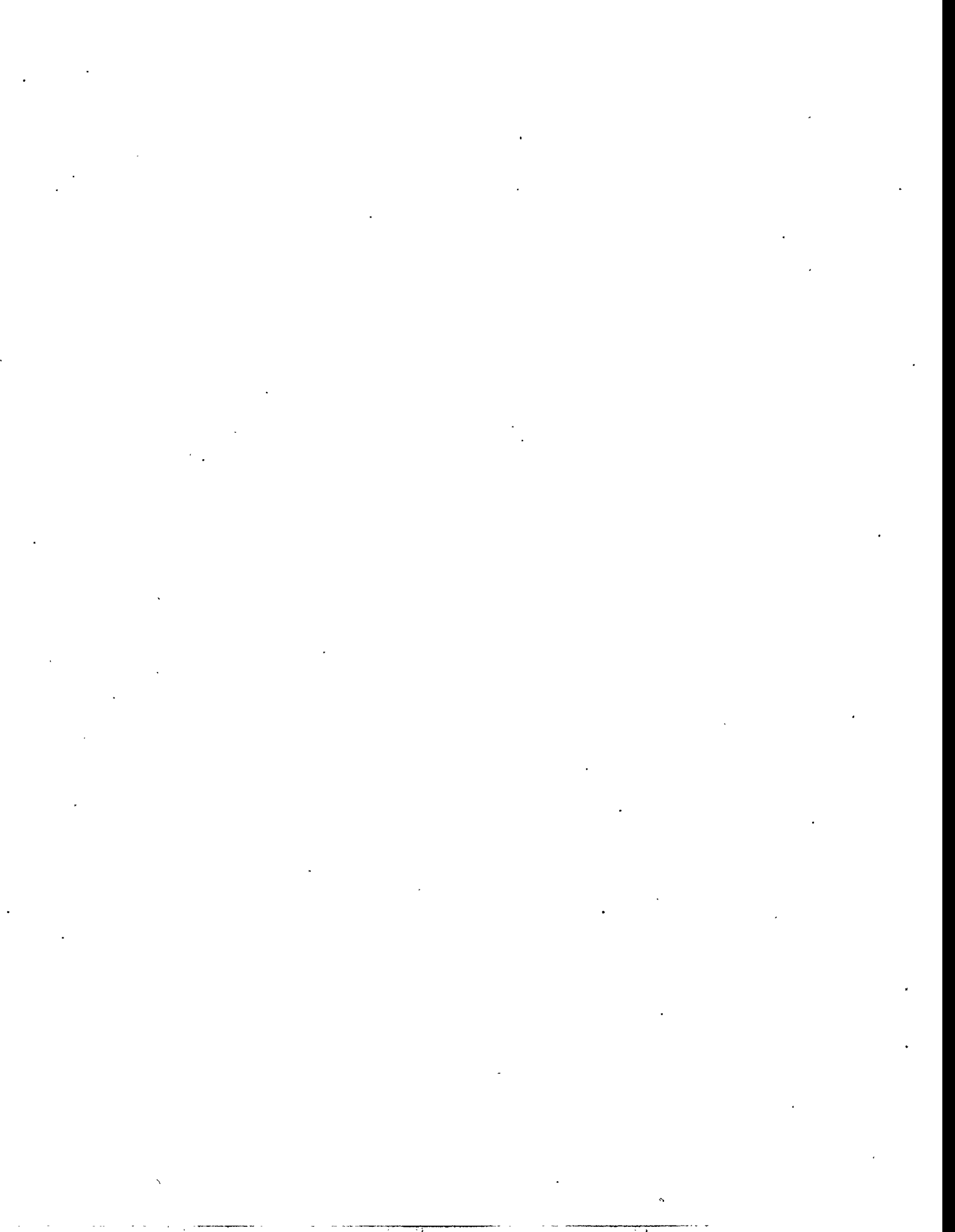
10.5 Closed-Loop System

The system was operated in a nearly closed-loop configuration. The air injected into the well by the blowers was recycled after being treated with the activated charcoal and then returned down the well for more stripping. Small additions of air, however, were required to balance the system. The closed-loop configuration was originally planned to minimize the amount of oxygen introduced to the

system and to conserve the amount of added carbon dioxide. Further, the closed-loop configuration is also intended to minimize the possibility of releasing the contaminant to the atmosphere. By reducing the amount of oxygen, biofouling and some inorganic precipitation problems are minimized. In the system at Edwards AFB, however, the aquifer was nearly saturated with oxygen and was not an oxygen sink for the system.

10.6 Condensation Effects

The estimated relative humidity in the exhaust air from the demonstration well is between 40% and 99%. Although the system has a water dropout configuration after it enters the treatment trailer, condensation still built up in the hoses outside the trailer. This was particularly true in the winter months, when there was a large temperature variation between ambient air temperature and exhaust air from the system. Approximately 25 to 500 mL of condensate water were drained out of the inlet and outlet air lines each morning during winter and spring. The water buildup overnight restricted the inlet airflow rate and, consequently, the pumping rate of the system. After the lines were drained, the system returned to optimum operating levels. Condensate water decreased as the ambient air temperatures increased to where there was no water accumulation in the summer months. To correct for condensation effects and minimize the maintenance caused by the condensation buildup, an in-line dryer, or water dropout vessel, is recommended for future field applications.



11.0 Performance Data

The demonstration was operated nearly continuously for 6 months (191 days) between January 16 and July 25, 1996. Postdemonstration sampling continued until the end of September 1996. The data gathered as a result of operating the in-well vapor-stripping system are presented in this chapter. The data describe the effectiveness of the system for cleaning up the aquifer or the reduction of TCE in the aquifer around the demonstration well. Other important elements described by the data include the zone of system influence, stripping ratios, and effects of the system on the subsurface.

11.1 Concentration Trends in Monitoring Wells

After 6 months of operation, the concentration of TCE was reduced significantly in the upper zones of the aquifer and to a lesser extent in the lower zones of the aquifer surrounding the demonstration well. The concentrations in the upper zones declined from a high that ranged from between 160 to 34 $\mu\text{g/L}$ to below the regulatory limit of 5 $\mu\text{g/L}$ in most of the monitoring wells around the demonstration well (Figure 11.1). The concentrations below the regulatory limit were also maintained for the duration of the demonstration. The rate of TCE decline was variable but, in general, was fastest in the wells nearest the demonstration well. In the lower zones of the aquifer between 45 and 50 ft below ground surface, the TCE concentration declines were detected in well M3d (deep), the well nearest the demonstration well in which the concentration fell from a pretest concentration of 290 to 173 $\mu\text{g/L}$ (Figure 11.2).

The rate of TCE concentration decline with respect to distance and depth indicated that the flow field may be asymmetrical, a result of the heterogeneous nature of the site geology in both the vertical and horizontal directions. The rate of decline in the shallow zones was most rapid in well M3s (shallow), the well nearest the demonstration well (10 ft crossgradient). The rate of decline was also relatively rapid in both M1s and M2s, the wells located 50 ft upgradient and downgradient from the demonstration well. The TCE concentrations in these three wells declined from between 133 to 85 $\mu\text{g/L}$ to below the regulatory limit of 5 $\mu\text{g/L}$. Wells M4s and M5s, located 30 and 50 ft crossgradient from the demonstration well, were not as responsive as M1s, M2s, or M3s. The TCE concentrations in wells M4s and M5s declined from 157 to 20 and 108 to 47 $\mu\text{g/L}$, respectively. This evidence indicated that the geology of the demonstration site is very heterogeneous, and the hydraulic conductivity was lower to the north of the demonstration well in the area of wells M4 and M5. Further evidence for the low hydraulic conductivity in this area was indicated by the rapid drawdown and slow recharge of well M4s during purging of the well for water sampling. None of the other shallow sampling zones had the same response. Conversely, based on the relatively rapid TCE concentration declines in wells M1s and M2s, a zone of relatively higher hydraulic conductivity was found between wells M1s and M2s.

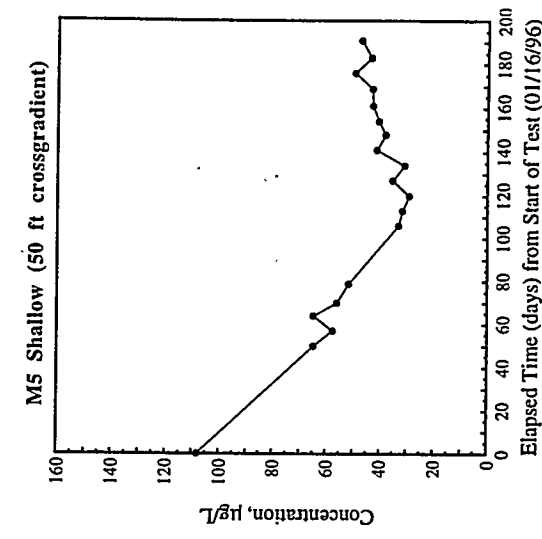
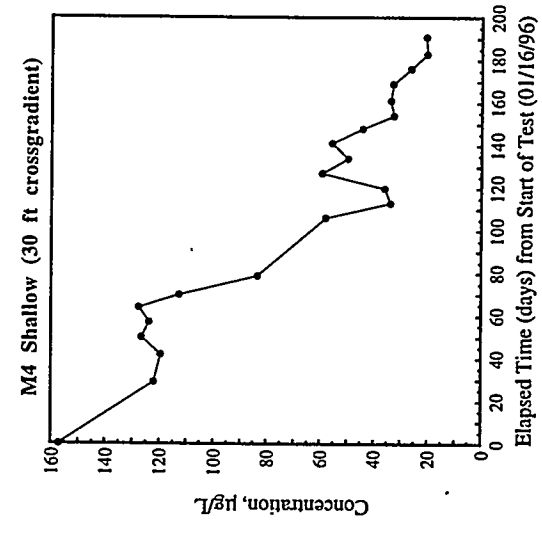
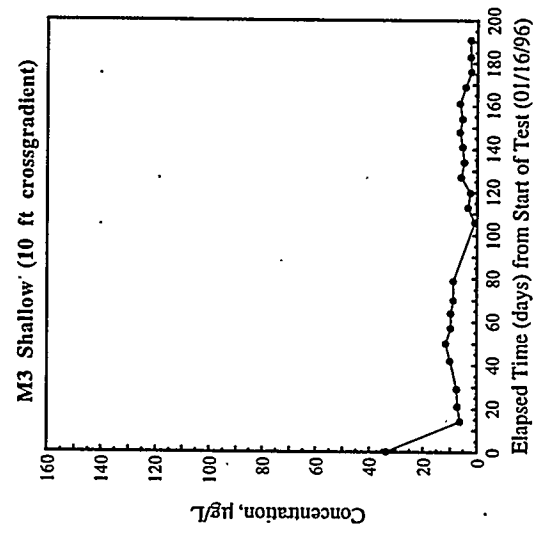
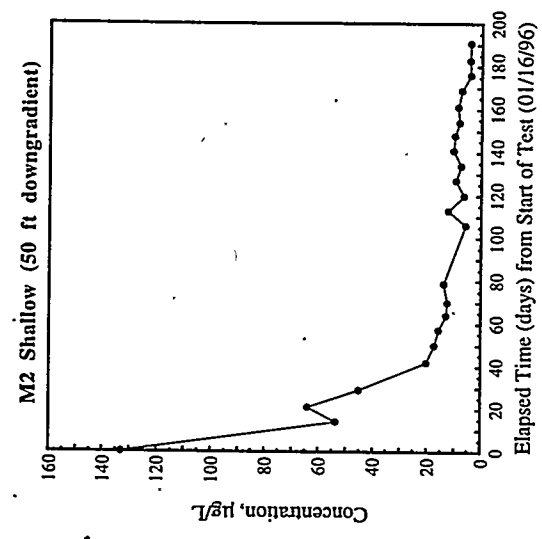
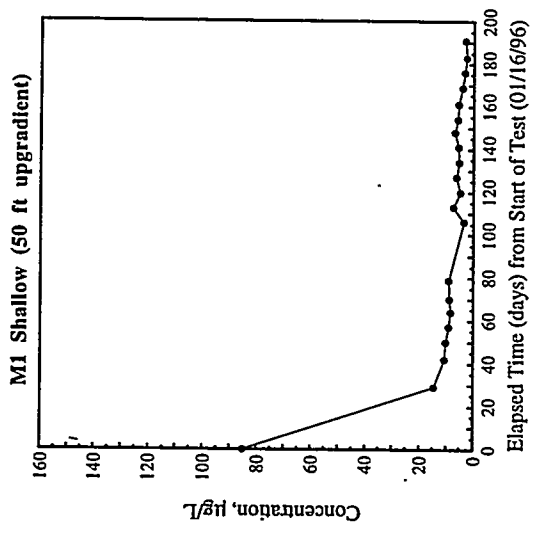
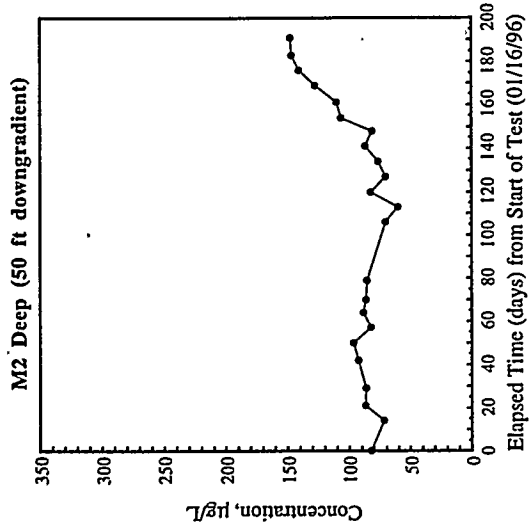
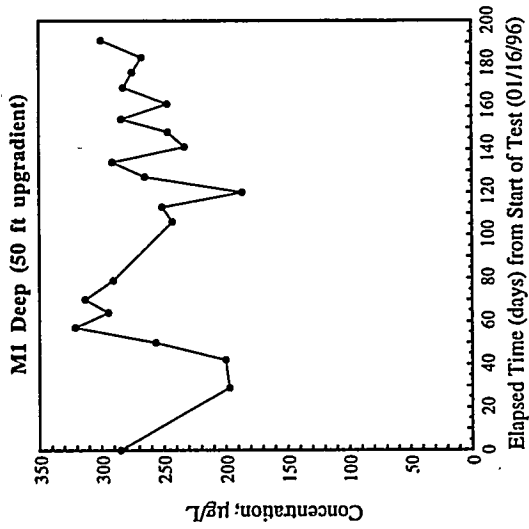


Figure 11.1. Trichloroethylene Concentrations in Shallow Monitoring Wells



11.3

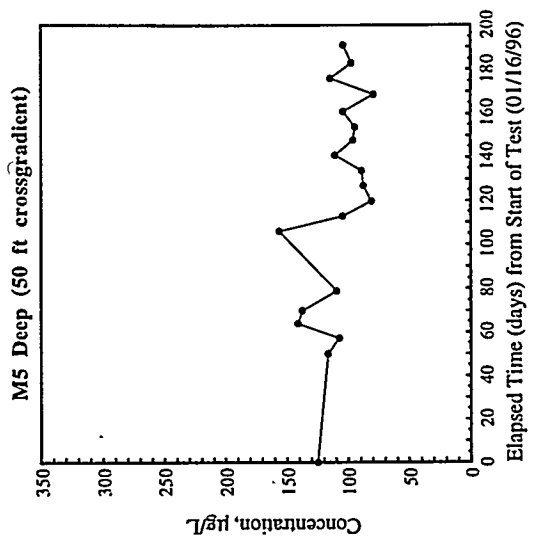
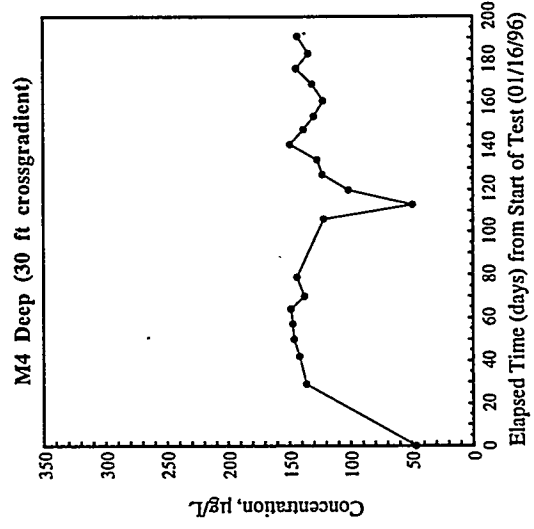
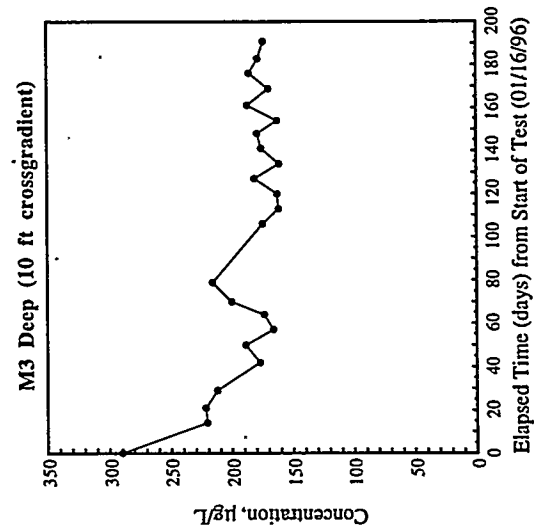


Figure 11.2. Trichloroethylene Concentrations in Deep Monitoring Wells

The concentration trends also indicated that the treated water was spreading at a greater rate horizontally than vertically. The concentration declines in the deeper (45- to 50-ft) zones were observed in well M3d, where the TCE concentration declined ~40% over the 6-month demonstration. However, TCE concentration declines were not as pronounced in the other deep zones (> 30 ft) from the demonstration well. This indicated that the rate of circulation into the lower zone was low (Section 11.2.1), and was attributed to the low-permeability zone identified in core at ~43 ft, which limited the percentage of water that recirculated. This zone at ~43 ft was relatively continuous across the site.

11.2 Zone of Influence

The zone of influence defined here is the area of aquifer that had a significant reduction in contaminant concentration and was determined primarily by the TCE concentration trends. Other indicators, such as the water-temperature trends and the groundwater-flow-velocity responses, were also used to define the zone. This zone of influence was strongly dependent on both site properties and system configuration.

The concentration profiles suggest the system's zone of influence was greatest in the shallow zone of the aquifer, where TCE declined in all the shallow monitoring wells located between 10 and 50 ft radially from the demonstration well. In the deeper zones of the aquifer, the TCE concentrations showed a notable decline in wells D2a at the intake screen and M3d, located 10 ft radially from the demonstration well. In the deeper wells located from 30 to 50 ft from the demonstration well, the concentration trends were not as apparent. But, when compared to the shallow well concentrations, there were indications that some of the treated water is reaching the lower zones of M4d and M5d (discussed more fully below). Data variability for wells M1d and M2d make any inferences of circulation influence at these sites highly subjective.

The flow-sensor data indicated flow-field changes as far as 35 to 50 ft crossgradient in the deep zone. The flow field measured at the flow sensors showed both horizontal and vertical flow velocities and azimuth changes in response to the pumping in the demonstration well (discussed in Section 11.7). The responses in the nearest flow sensor (F3) were most responsive and decreased with distance from the demonstration well. The farthest flow sensor (F1), at 50 ft crossgradient to the demonstration well, showed a very slight response to pumping in the demonstration well.

11.2.1 Recirculation

The zone of recirculation defined here is the area developed by the in-well vapor-stripping system in which the treated water outflow is recycled back through the intake for another pass through the stripping system. The zone of recirculation was estimated by using a mass-balance relationship to qualitatively assess the percentage of recirculated water. From these estimates, the zone of recirculation may extend beyond 30 ft from the demonstration well.

Contaminant mass-balance relationships can be used semiquantitatively to assess the percentage of recirculated (TCE-reduced) water within groundwater extracted at well D2a (inlet). The basic mass-balance relationship that relates removal of TCE from the in situ well-sparging circulation-cell system can be expressed as:

$$M_r = M_i - M_o \quad (11.1)$$

where M_r = mass flux of TCE removed/stripped at well, M_i = mass flux of TCE at well inlet, and M_o = mass flux of TCE at well outlet.

The mass of TCE at the inlet, M_i , is equal to the sum of TCE masses provided by the formation, M_f , and the mass supplied by the recirculated water, M_{rc} . It should be noted that at and in proximity to well D2a, M_{rc} is assumed to equal M_o . The mass flux, M , of TCE at the respective locations is a product of the discharge rate, Q , multiplied by concentration, C . For example at the inlet, $M_i = Q_i C_i$ and, similarly, at the outlet, $M_o = Q_o C_o$. By substitution, the TCE mass flux at the inlet can be written as:

$$M_i = M_f + M_{rc} \quad (11.2)$$

or

$$Q_i C_i = (Q_f C_f) + (Q_{rc} C_{rc}) \quad (11.3)$$

Noting that $Q_i = Q_f + Q_{rc}$ and if the recirculation ratio, R , is defined as being equal to Q_r/Q_{in} and $Q_f = (1-R)Q_{in}$; then substituting these relationships into Equation (11.3), Equation (11.3) can be rewritten and reduced to:

$$C_i = C_f (1-R) + C_{rc} R \quad (11.4)$$

Rewriting Equation (11.4) as an expression of the recirculation ratio yields:

$$R = (C_f - C_i)/(C_f - C_{rc}) \quad (11.5)$$

Theoretically, Equation (11.5) indicates that the percentage of recirculated water at the well D2a inlet can be determined directly (without knowledge of the injection/extraction rate); however, to be used quantitatively, the concentration, C , values must be known precisely with time. Of the concentration inputs in Equation (11.5), the TCE mass within the formation, C_f , is the parameter most poorly defined (i.e., the exact undiluted TCE concentration provided by the formation to the inlet during the flow circulation). Existing spatial distributions suggest the presence of concentration heterogeneity both laterally and vertically within the formation (i.e., in response to the presence of plume patterns), which would be expected to change with time during the duration of the circulation test. This limitation severely restricts the possible use of Equation (11.5) for quantitative applications.

Realizing these limitations in determining the percentage of recirculated water, Equation (11.5) was employed only as a semiquantitative assessment. To proceed with the recirculation calculation, the following TCE concentration estimates were used:

- $C_f = 97.1 \mu\text{g/L}$; based on average of D2a inlet pretest values (Figure 11.3)
- $C_i = 40.7 \mu\text{g/L}$; based on average of D2a inlet late-time test values (test interval 120 to 191 days; see Figure 11.3)
- $C_{rc} = 4.8 \mu\text{g/L}$; based on average of D2a outlet late-time test values (test interval 120 to 191 days; see Figure 11.3).

Substituting these TCE concentration input values into Equation (11.5) yields an estimate of recirculated water of 61% of the total inflow at well D2a. It should again be realized that this is a semiquantitative estimate and could be in error by $\pm 20\%$ (or more) because of the uncertainties in actually knowing C_f .

Equation (11.5) in the strict sense can be applied only to pumping/injection wells, but is used in this case to semiquantitatively assess the percentage of recirculated water at other well sites surrounding recirculation well D2a. For this assessment, concentration data from wells M3d and M4d (located 10 and 30 ft crossgradient from well D2a) were utilized. Table 11.1 lists the concentration data values used at each site and the associated recirculation calculation based on Equation (11.5). For these wells, C_f and C_i values were estimated using the pretest and late-time concentration data at the respective well sites. C_{rc} values were estimated using the late-time concentration data for the respective overlying shallow wells (i.e., M3s and M4s). As shown in Table 11.1, estimated values of recirculated water at wells M3d and M4d were 44% and 25%, respectively. Again, it should be noted that a high level of uncertainty is associated with these percentage estimates; however, the decreasing trend away from the circulation well is consistent with expected conditions and also suggests that the "area of influence" may extend beyond 30 ft in this direction at the demonstration site. This is also corroborated by flow sensors F1, F2, and F3, located approximately along the same azimuth (i.e., north-south direction) at distances of up to 50 ft, which showed head and flow responses associated with the flow circulation test.

11.3 Pumping Rates

The pumping rates of the system are a function of the submergence-to-lift ratios, injected air volumes, pipe diameters, and formation properties. At the beginning of the demonstration, the pumping rate was limited by the infiltration capacity of the vadose zone; the aquifer could produce more water than what the upper zone could accept. The formational limitations of the upper zone required that the system be operated at relatively low flow rates (~2.5 gpm). These flow rates were lower than expected when planning the project but were within the range of other flow rates measured at the site. Although not at this site, it is possible with airlift pumping to pump at rates of 150 gpm or more (Driscoll 1986).

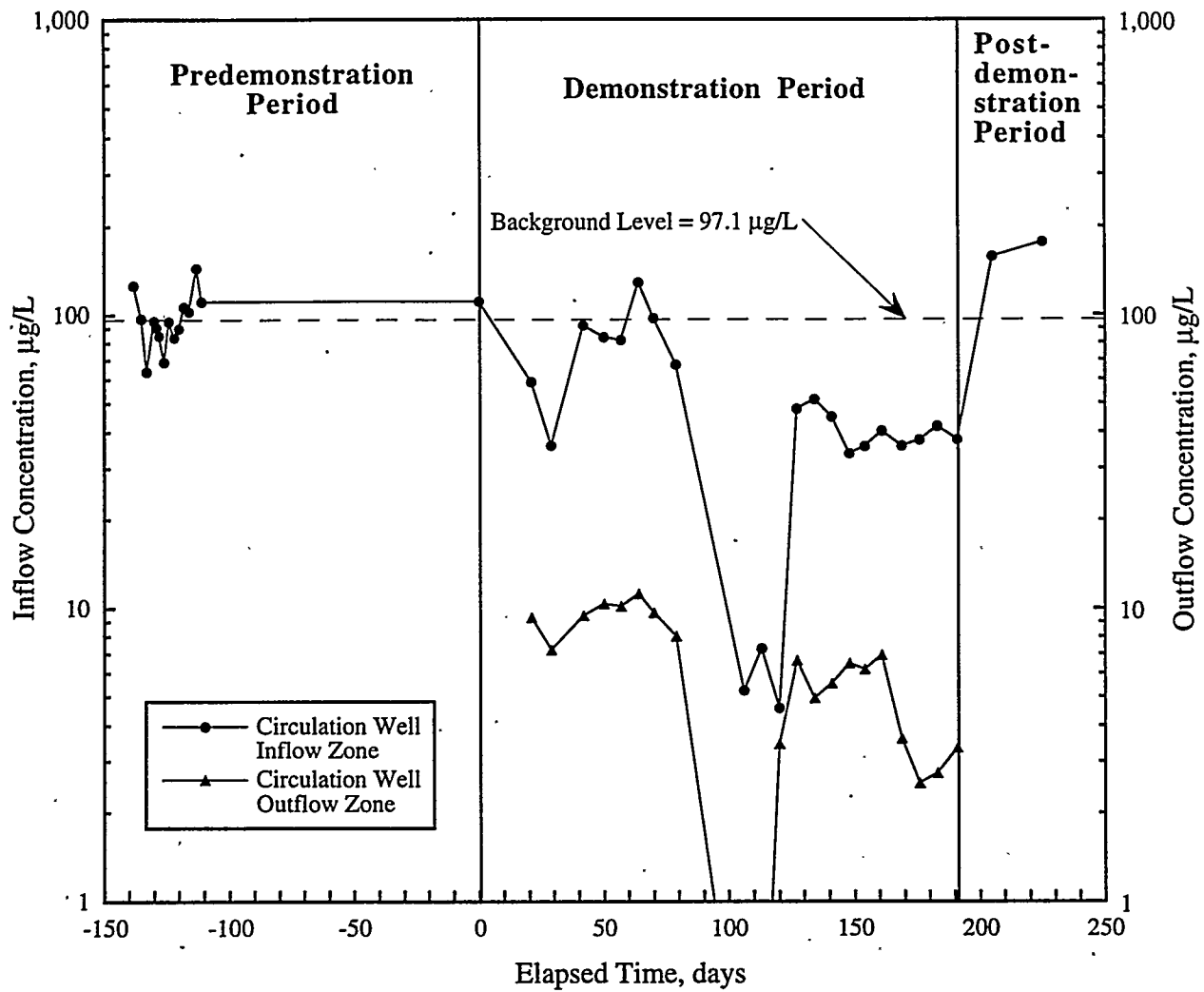


Figure 11.3. Concentration Profiles for Estimating Recirculation

Table 11.1. Recirculation Rates

Well Site	C_f	C_i	C_{rc}	Recirculation Rate, R	Distance from Demonstration Well, ft
D2a (inlet)	97.1	40.7	4.8	61%	0
Well M3d	307.1	173.2	4.8	44%	10
Well M4d	167.2	135.3	37.2	25%	30

Between January and April of the demonstration, the air-injection rates were slowly increased. The return heights were essentially steady at 17 to 18 ft above the base of the upper screen, or 2 to 3 ft below ground surface. The air-injection rates were increased during the first months of the demonstration as a result of increasing infiltration rates in the upper zone. The increase in infiltration rates may be the result of several factors, including saturation of the zone around the well and maintenance of the soil properties with calcium chloride (see Section 10.3). The flow rate estimated in the well in April was 10 gpm based on a reinfiltration test of the upper zone. After the system was reconfigured with a third blower and the air-injection point raised, the estimated pumping rate was 7 to 8 gpm based on the air-injection rates and water-level drawdowns in the adjacent wells.

11.4 Airflow Rates and Stripping Ratio

The airflow rates and the resulting stripping ratios were determined based on the system's configuration. Two basic system configurations were used during the demonstration. The system configuration was held constant from January to April and again between June and July. In May, the system was being reconfigured. During the earlier period (January to April), the air-injection point was maintained at a 20-ft submergence (47-ft depth) and 28-ft lift, while the air-injection rates were adjusted to maintain the return heights, or ponding heights, in the 10-in. annulus. The estimated pumping rate in April was 10 gpm based on a reinfiltration test.

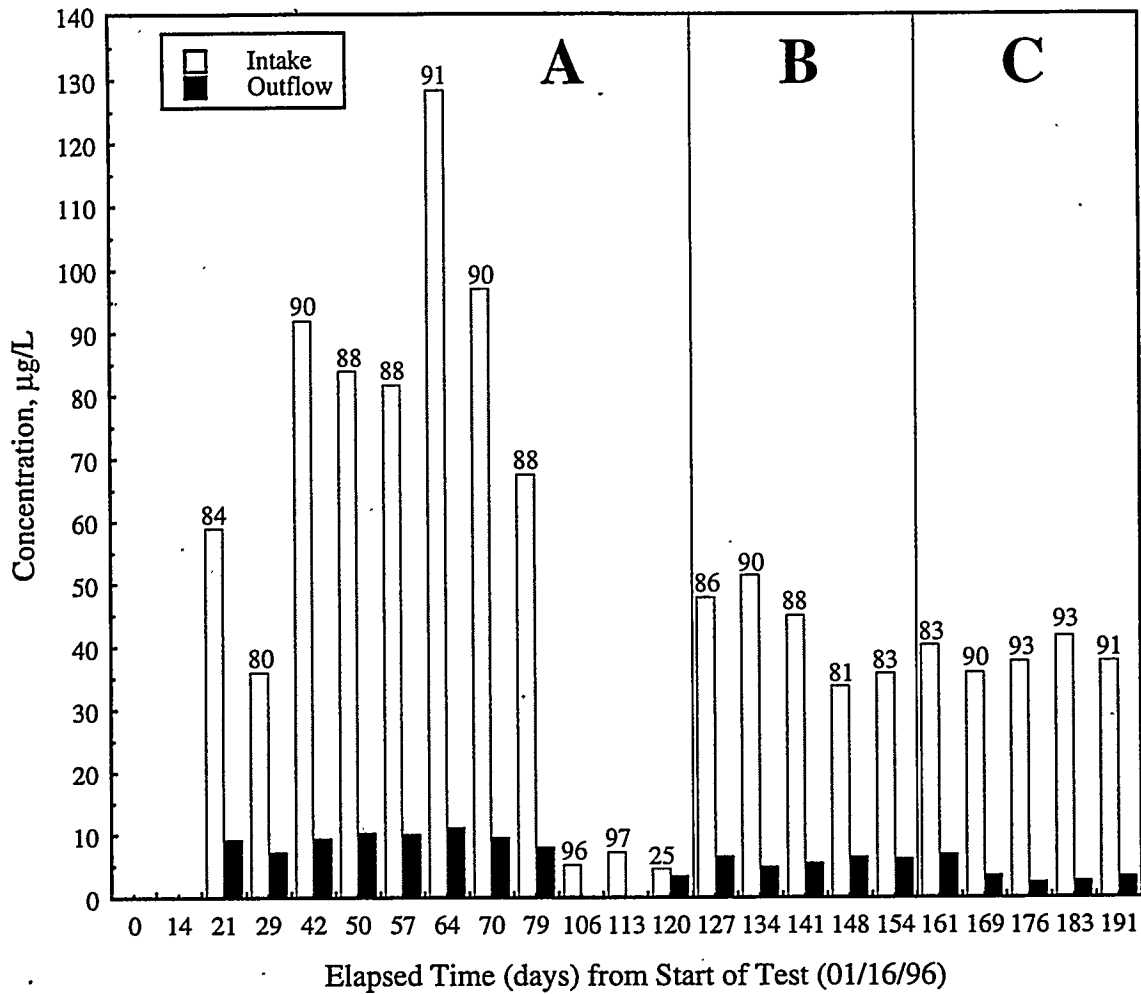
The system configuration was changed in late April/early May. A third blower was added to increase the air-injection rates, and the air-injection depth was raised to provide higher air-to-water ratios. The objective was to increase the stripping ratio and bring the TCE values in the aquifer to below the regulatory limit. During this period, the airflow rate was ~60 scfm, the air-injection depth was 8.5 ft, and the resulting pumping rate was ~7 to 8 gpm.

The stripping ratios determined from TCE analyses of water samples from the inlet and outlet of the treatment well averaged 89% between February 14 through April 4 (Figure 11.4). The water-flow rate during this period was estimated to be ~10 gpm, and the air-to-water ratio was ~29:1. Samples collected between June 25 and July 25 yielded an average stripping rate of 90%, with individual rates ranging from 82.8% to 93.4%. During the June to July period, the system ran at an estimated pumping rate of 7 to 8 gpm, slightly lower than the estimated 10 gpm observed earlier in the demonstration, and the air-to-water ratio was higher, at ~53:1.

An encouraging result of the demonstration was the higher-than-expected stripping rates of the system. In the laboratory testing, a 7.5:1 air-to-water ratio provided 50% stripping of a similar constituent, 1,1,1-trichloroethane (Gilmore and Francois 1996).

11.4.1 Theoretical Stripping Rates

Observed VOC stripping rates for the period June 25 through July 25 were compared to stripping rates calculated using the theoretical airlift-pumping and mass-transfer model (Francois et al. 1996) in Table 11.2. The theoretical estimates compared favorably with the observed rates.



A: Air-injection depth 22 ft below initial water table, 2 blowers operating.
 B: Air-injection depth 9.0 ft below initial water table, 3 blowers operating.
 C: Air-injection depth 8.5 ft below initial water table, 3 blowers operating.

Figure 11.4. Intake and Outflow Concentrations with Stripping Ratios

Table 11.2. Comparison of Measured and Theoretical Stripping Rates

Time Period	Pumping Rate, gpm	Airflow Rate, scfm	Air:Water Ratio	Upper Limit on Theoretical Stripping Rate, %	Stripping Predicted by Airlift Model, %	% Difference from Measured Values
Jan -	10	34.0	25.5	90	87	-2%
Apr	10	43.9	32.8	92	90	+1%
Jun -	7	46.6	49.8	94.9	94.0	+4%
Jul	8	61.9	57.9	95.6	94.6	+5%

There was no attempt to model the VOC stripping rates for January through April. During this period, there were several key parameters whose values were uncertain. The airflow meter may have been adversely affected by low temperatures and condensate water during the winter months, resulting in anomalously low reported airflow rates. Initially, the system was shut down briefly several times to clear condensation of water in the air lines. There is also some uncertainty in the pumping rates. All of these uncertainties, however, were mitigated or eliminated for the second half of the demonstration (May through July). A stable period of operation during late June and July was used for comparing theoretical and observed stripping rates.

The key parameters used in the airlift-pumping model are as follows:

- air-injection depth 8.5 ft below initial water table
- drawdown 2.2 to 2.5 ft
- starting lift 18 ft
- eductor pipe inner diameter 4.0 in.
- air line outer diameter 1.9 in.
- water temperature 20°C
- Henry's Constant for TCE at 20°C 0.35.

The values for drawdown were conservative and did not include additional head losses that occurred between the extraction screen and the sparger (e.g., head loss across the orifice plate used for measuring water-flow rate within the well). These losses were relatively minor, however (on the order of several inches). The starting lift used in the model (18 ft) was slightly lower than the minimum starting lift (22 ft). This was necessary to attain the observed pumping rates (7 to 8 gpm).

As noted above, the theoretical and observed VOC stripping rates were in relatively close agreement. The model overestimated the observed stripping rates by 4% to 5%. The predicted airflow rates (46.6 and 61.9 scfm) were similar to the range of observed airflow rates (55 to 65 scfm). These were very encouraging because the responses of the airlift system to changes in certain key parameters (e.g., pumping rate, starting lift) were nonlinear.

11.5 Groundwater Mound Development from Recharge

Three piezometers around the demonstration well monitored the development of the predicted groundwater mound as a result of the reinfiltrating water. The water-level readings from the piezometers indicated that the groundwater mound was asymmetrical. Two piezometers, each 5 ft from and on either side of the demonstration well, showed very different mound development. Piezometer P1 on the south indicated a water-level increase of over 4 ft, while piezometer P3 on the north showed an increase of just over 1 ft. A third piezometer, P2 located 10 ft to the west of the demonstration well, showed an increase of 0.6 ft (Figure 11.5). In addition, piezometer P1 was the most responsive of the three, responding rapidly to the changes in system operation. The groundwater mound continued to increase over the first 60 to 70 days of the demonstration. This gradual increase is in part attributed to the increasing pumping rate in the demonstration well and, hence, the increasing amount of water

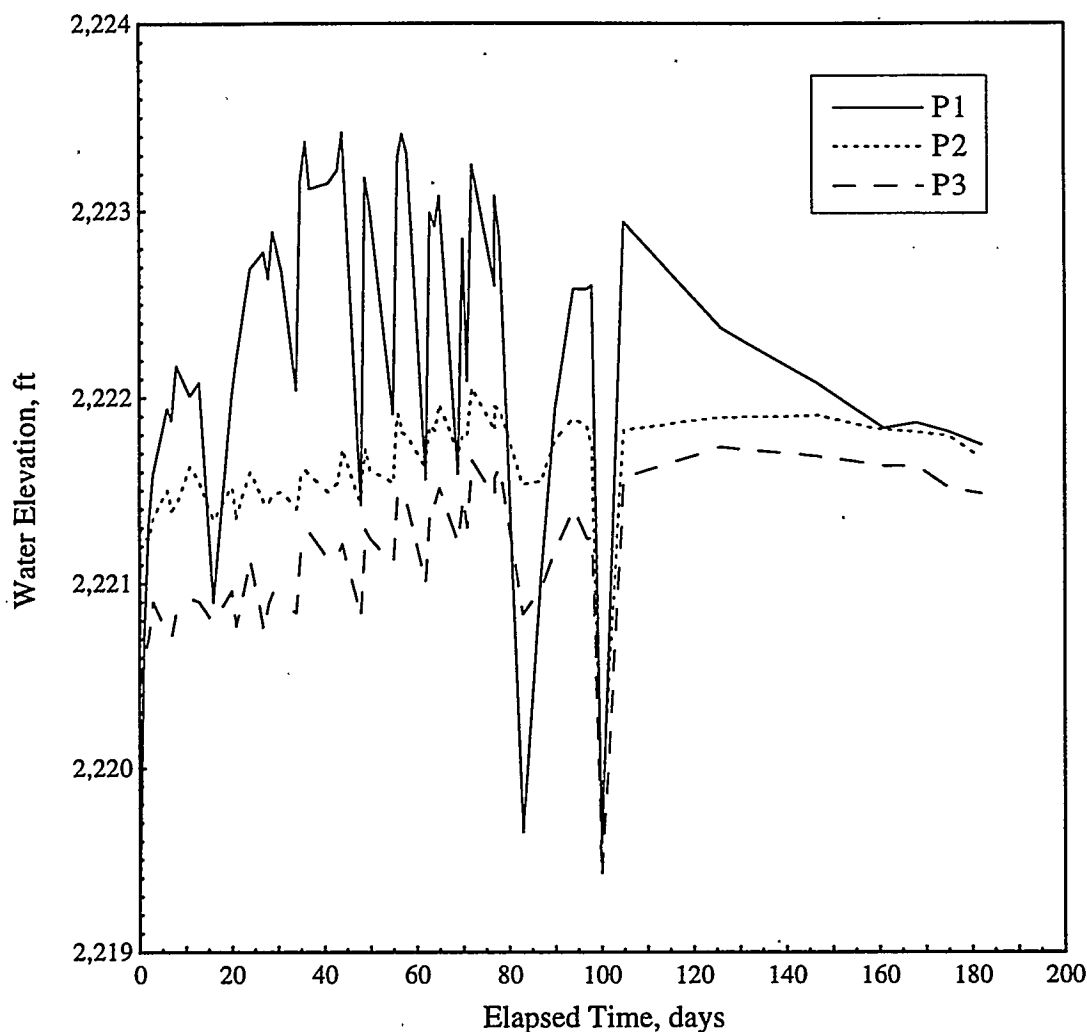


Figure 11.5. Piezometer Water Levels

reinfiltrating back to the water table. Following the reconfiguration of the system, from ~110 days to the end of the demonstration, the system was stable. The pumping rate was held at a lower 7 to 8 gpm. During this time, the water level in P1 decreased to approximately the level in P2 and P3, indicating a flatter and more symmetrical groundwater mound.

The STOMP simulations of the system predicted a symmetrical groundwater mound at a level of ~1.8 ft located 5 ft from the well. This is between the actual readings at P1 and P3, which is further evidence of the geologic heterogeneity at the site.

The initial asymmetry of the groundwater mound could be the result of a combination of the heterogeneity at the site and, possibly, the piezometer construction. A relatively low-permeability zone was identified at 29 ft in core from wells C1 and D1 but was not continuous across the site. Because

detailed geology was not available from the piezometer wells, it could only be speculated that the differences in the water levels in the wells were attributed to the geology.

11.6 Postdemonstration Concentration Trends

The TCE concentration trends after the pumping was stopped in the demonstration well varied at each monitoring point but, in general, there was a notable increase in concentration at each monitoring well completed in the upper part of the aquifer (Figure 11.6). This response is most apparent for wells located farthest from the demonstration well: M1s, M2s, and M5s, all of which are 50 ft from the demonstration well. M1s showed the most rapid response of all. This was attributed to its being located near the upgradient limit of the zone of injection for the system. As soon as pumping ceased,

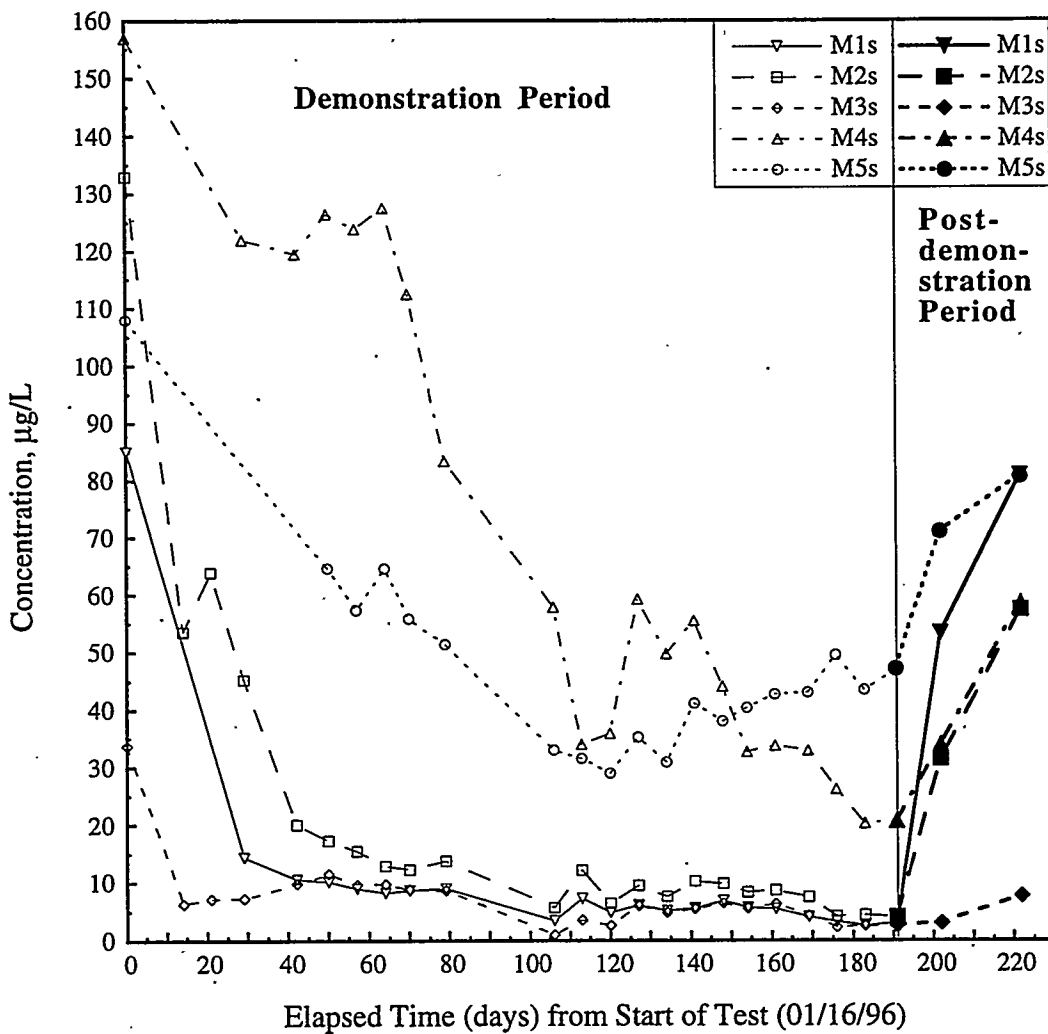


Figure 11.6. Shallow Monitoring Well TCE Concentrations Versus Elapsed Time

contaminated water from outside the zone began to flow downgradient toward M1s; hence, the response was very rapid. Similar reasoning could be applied to the response at M5s, which is cross-gradient of the demonstration well. The response observed at M2s was not readily apparent; it might be expected that relatively clean water upgradient of M2s would continue to migrate beyond this well for a fairly long period of time. This does not seem to be happening, however. The response at M3s and M4s was slower than at the other locations because these wells are closer to the center of the cleanup zone.

The monitoring wells in the deep part of the aquifer showed no appreciable change in concentration during the demonstration, with the exception of the intake of the demonstration well and the possible exception of monitoring well M3d (Figure 11.7). The concentration at the intake of the demonstration well rebounded very quickly and might be attributed to its being located in a zone of recirculation

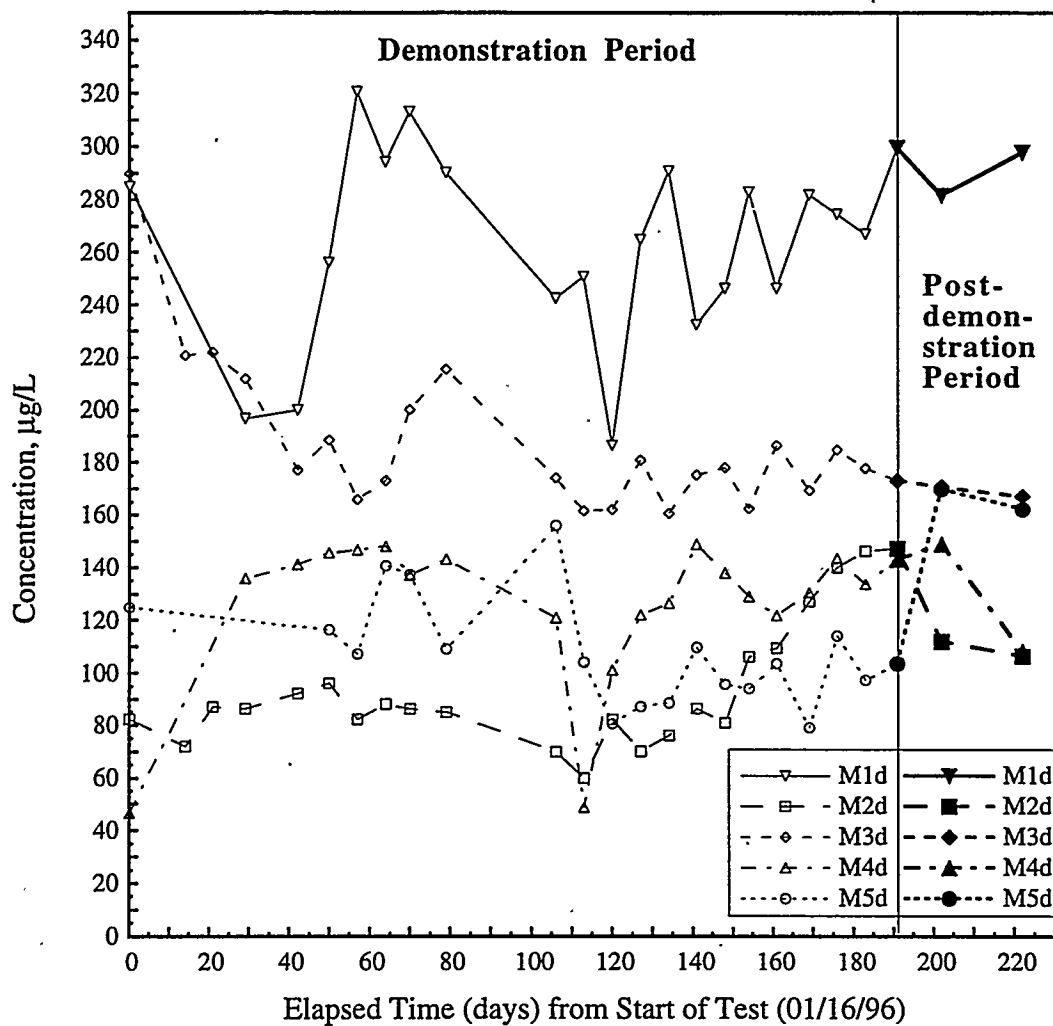


Figure 11.7. Deep Monitoring Well TCE Concentrations Versus Elapsed Time

whose spatial extent was rather limited (this was discussed in greater detail in Section 11.2.1). Well M3d, which showed a possible decrease in concentration as a result of recirculation, showed no response to the cessation of pumping.

Wells M1d, M3d, M4d, and M5d showed no appreciable response to either the demonstration itself or the cessation of pumping.

11.7 In Situ Permeable Flow-Sensor Results

The flow-velocity data as a function of time from the sensors are illustrated in Figures 11.8, 11.9, and 11.10. The time axis is in days, with time zero being January 16, 1996, the day that the demonstration was started. Despite the fact the measured flow velocities were quite low relative to the range of flow velocities that the sensors were designed to measure, several notable events were apparent in the data. When the sensors were initially activated in early August 1995 (around day -160), the demonstration well was being tested for the first time. This caused significant perturbations to the flow velocity at all three sensors. At F3 and F2, the sensors closest to the demonstration well, the primary effect was a downwardly directed pulse of flow and a reduction in the magnitude of the horizontal component of flow.

Following the initial test, there was no activity at the site that influenced the hydrologic conditions in the lower aquifer until late November/early December (day -50 in Figures 11.8, 11.9, and 11.10), when the demonstration well was developed. At that time, water was pumped both into and out of the lower aquifer through the lower screen, with pronounced effects on the flow velocity measured at the two closest flow sensors. There was only a hint of an effect at sensor F1, the farthest sensor from the demonstration well.

During December 1995 and early January 1996 (days -33 to 0), the demonstration well was briefly tested on several occasions, with measurable effects on the lower aquifer detected by sensors F3 and F2. On January 16, 1996 (day 0), when the demonstration was started and run continuously for ~6 months, the effect was measurable at all three flow sensors. The most pronounced effect was a downwardly directed vertical component of flow that was detected immediately by sensors F2 and F3. The relative responses in each of these flow sensors are believed valid; however, the absolute magnitude was probably amplified over what the natural vertical flow component was in the formation. The relatively large vertical flow component was likely the result of sensor installation (i.e., allowing the formation to collapse as the drill string was extracted). This likely created a conduit of relatively high permeability between the upper and lower portions of the aquifer. As the hydraulic head in the upper aquifer increased because of the formation of the groundwater mound around the demonstration well, flow was induced down these high-permeability pathways.

The vertical component of flow measured by sensor F1 was not initially influenced by the demonstration; however, after day 90, a downward component of flow began to increase at 50 ft from the demonstration well. This delayed effect may reflect the horizontal growth of the mound during the progress of the demonstration.

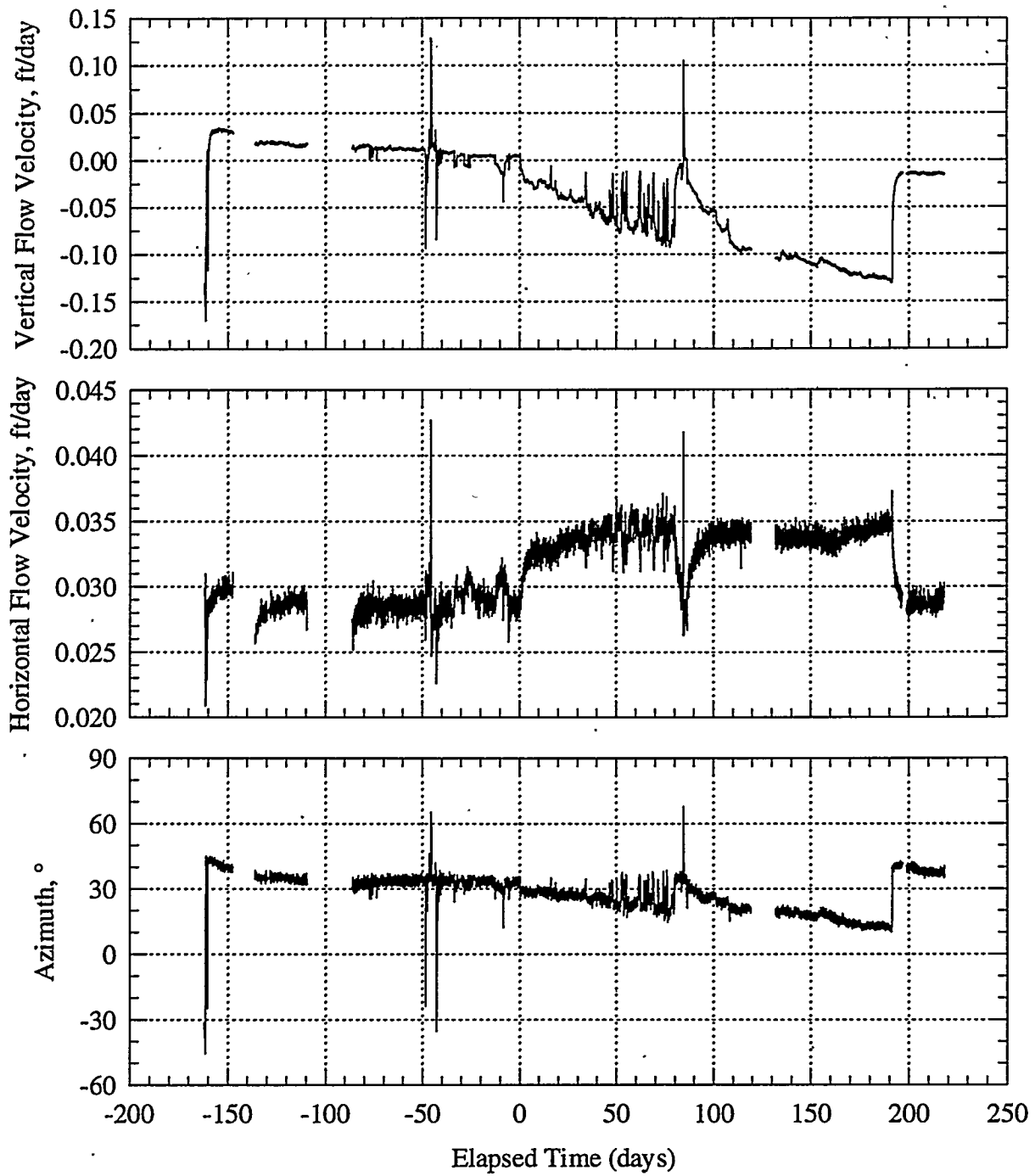


Figure 11.8. Flow Velocity as a Function of Time Observed by Flow-Sensor F3 (17.5 ft radially from demonstration well)

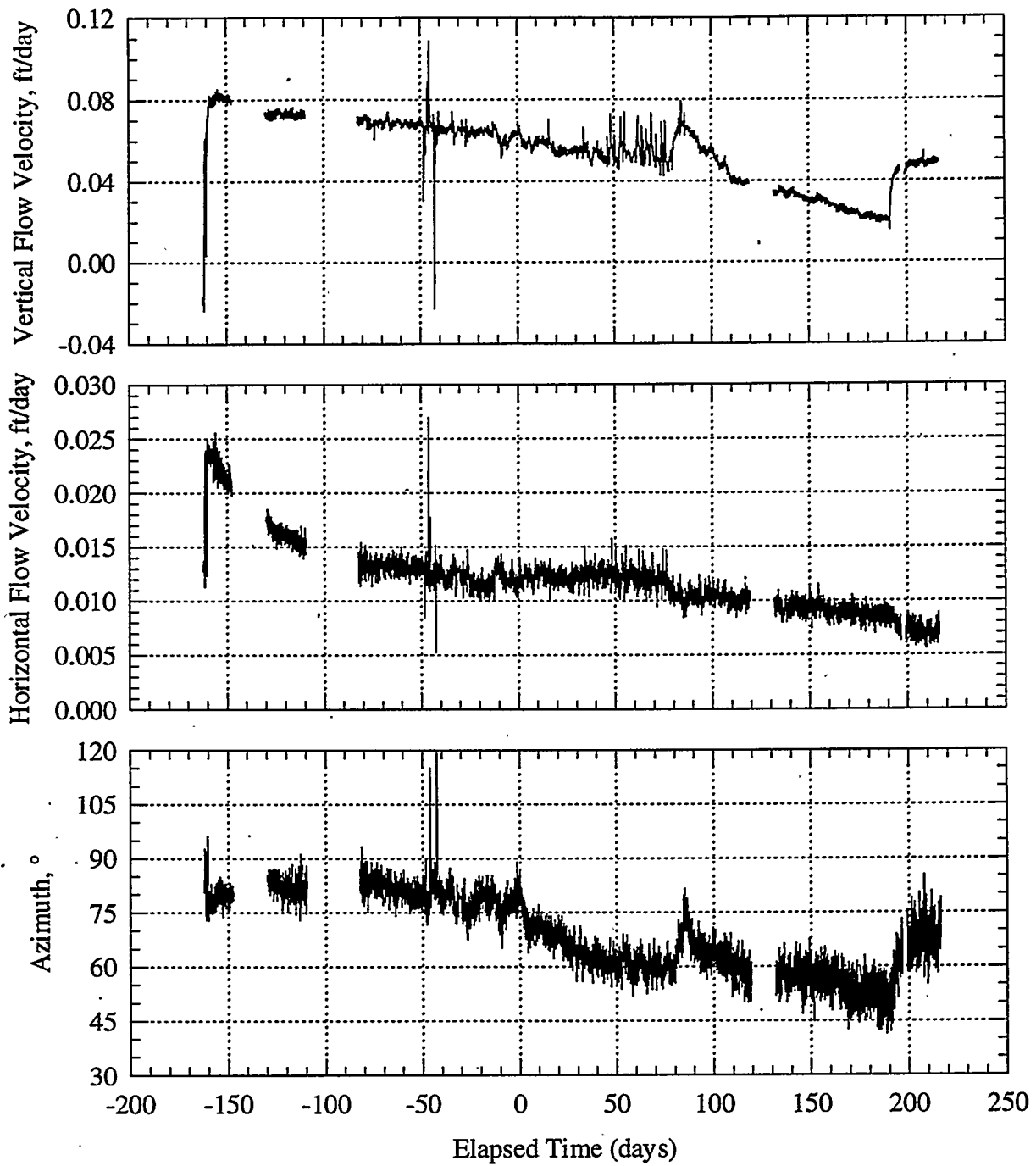


Figure 11.9. Flow Velocity as a Function of Time Observed by Flow Sensor F2 (34.5 ft radially from demonstration well)

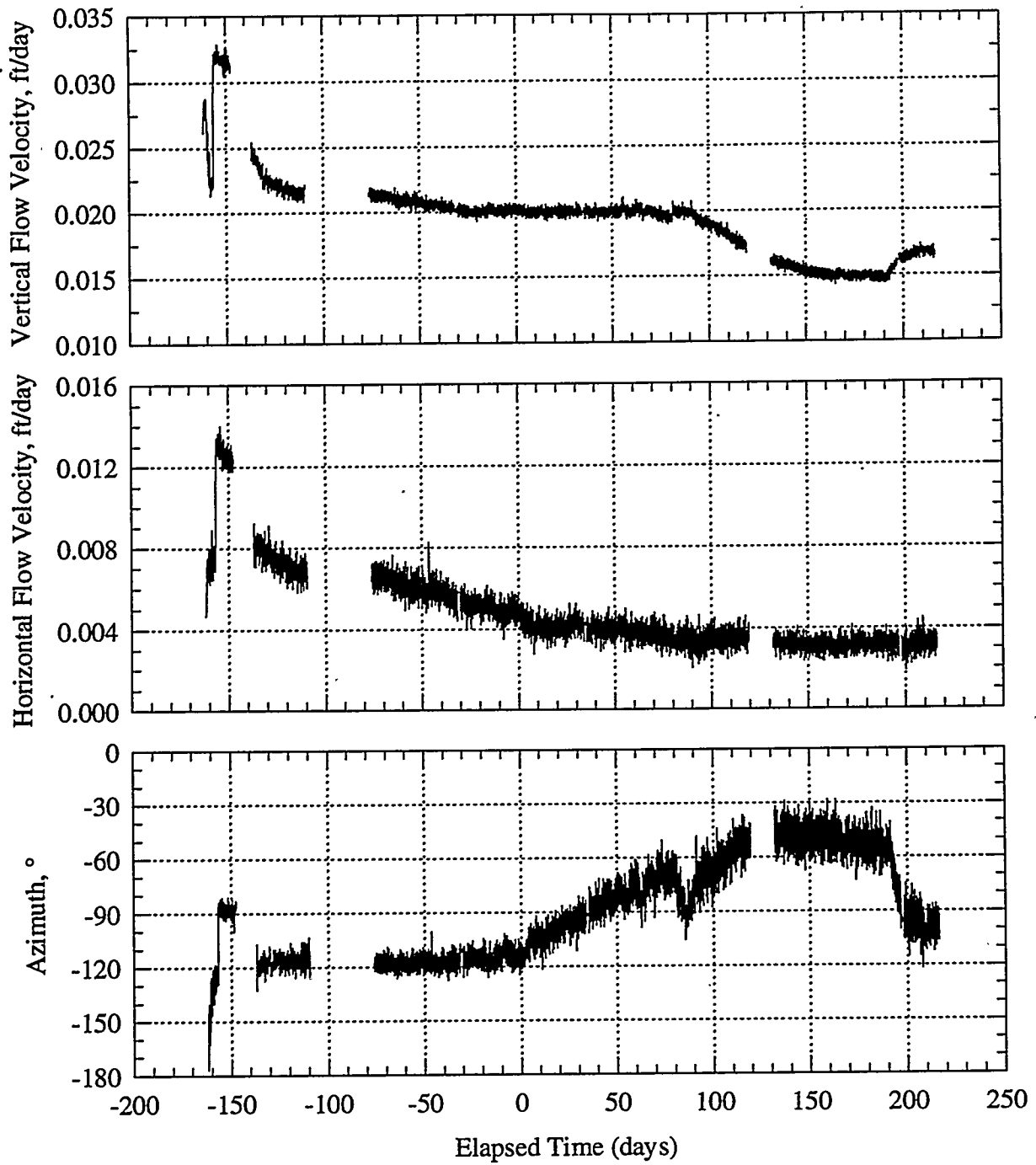


Figure 11.10. Flow Velocity as a Function of Time Observed by Flow Sensor F1 (50 ft radially from demonstration well)

The horizontal component of the groundwater-flow velocity was also affected by the demonstration. Figure 11.11 is a map view of the site that shows the direction and magnitude of the horizontal component of the flow velocity measured by the flow sensors immediately prior to the start of the demonstration, immediately prior to the end of the demonstration, and 1 month after the end of the demonstration. While the changes in flow velocity observed during the demonstration were apparent

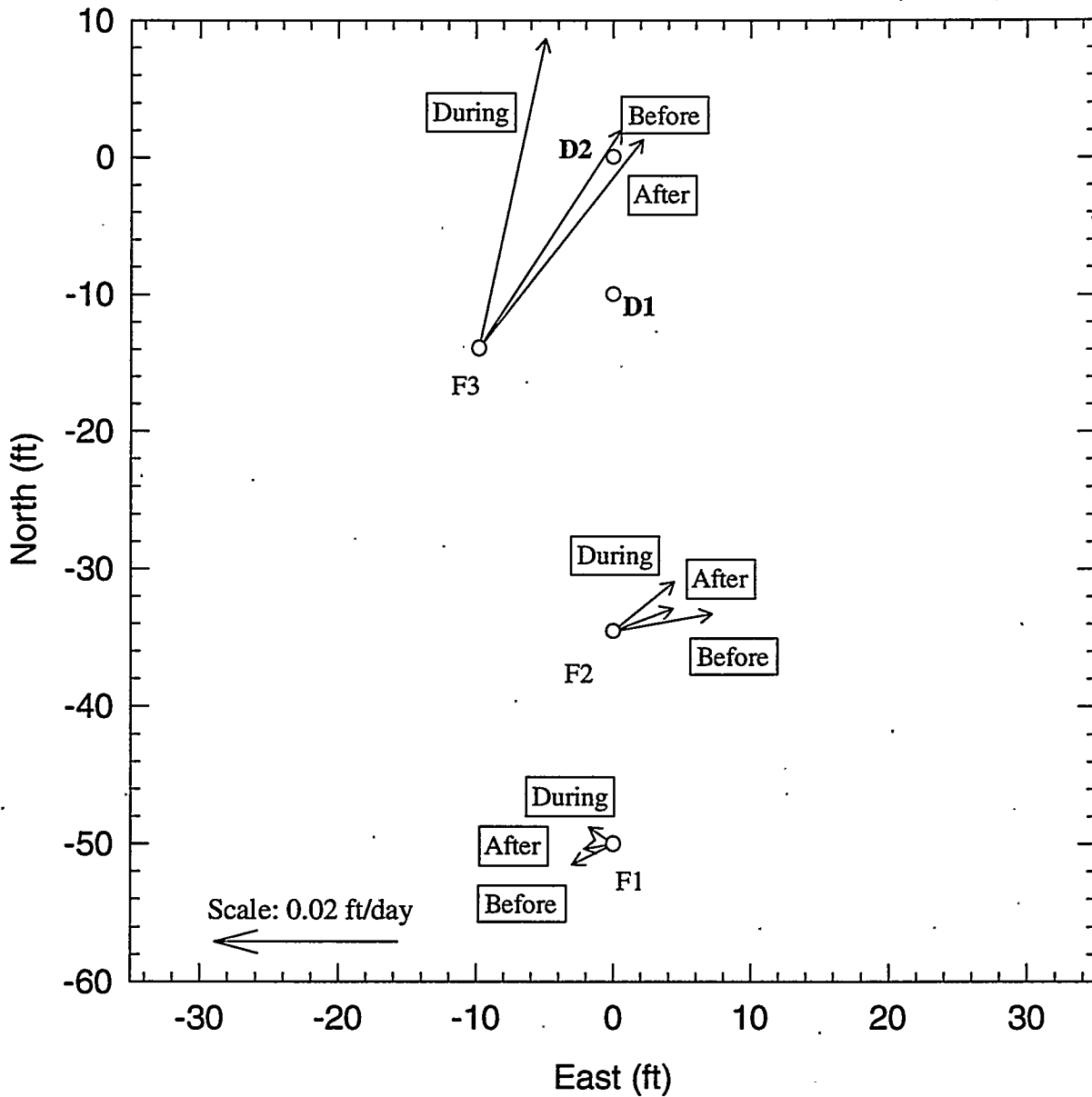


Figure 11.11. Measured Flow-Velocity Vectors (horizontal component)

in the raw data, the changes in the groundwater-flow regime attributable to the demonstration could be isolated by subtracting the background flow velocity at the site from the raw velocity data (Figure 11.12). The background velocity subtracted was the velocity measured by each sensor just prior to the initiation of the demonstration (days -20 to -13).

At F3, the horizontal flow velocity, which was directed toward the demonstration well even before the demonstration started, increased in magnitude when the demonstration started. During the course of the demonstration, the direction of the horizontal component rotated counterclockwise away from the demonstration well. At the conclusion of the demonstration, the flow velocity returned to its pre-demonstration direction and magnitude.

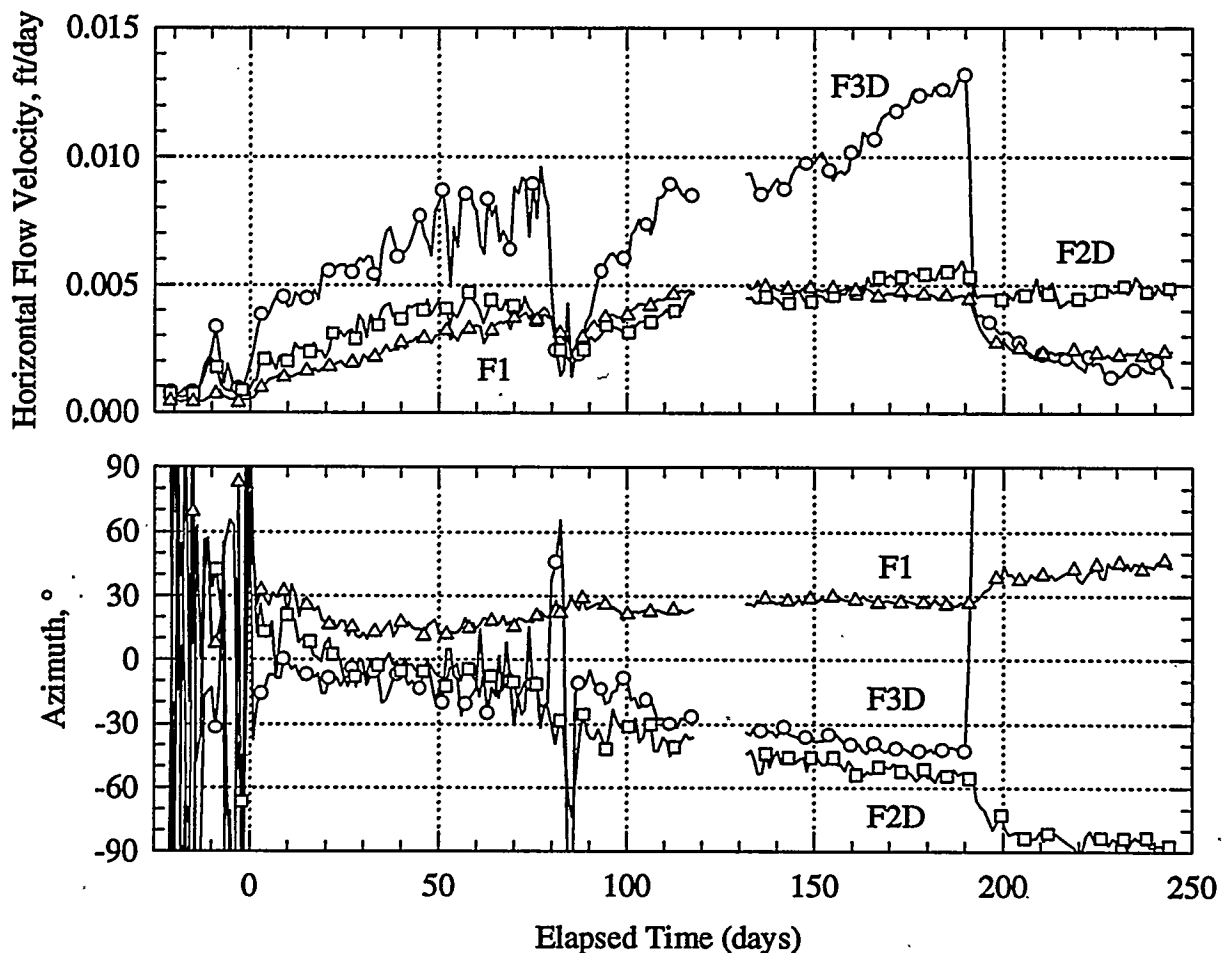


Figure 11.12. Horizontal Components of Flow Velocities Measured by Three Flow Sensors after Subtraction of Background Flow Velocities

At F2, the horizontal component of flow was directed toward the east prior to the start of the demonstration. This was the direction of the expected background flow velocity at the site. When the demonstration started, the direction of the horizontal flow velocity rotated counterclockwise by ~20 degrees. This reflected the superposition onto the background flow of a horizontal flow vector directed toward the demonstration well. As the demonstration progressed, the magnitude of the superimposed horizontal component increased steadily for the first few months, which corresponded to the time when the pumping rate in the demonstration well was increasing, then leveled off for the last few months of the demonstration when the pumping rate remained relatively constant. When the demonstration was terminated, the direction of the flow velocity rotated clockwise away from the demonstration well, reflecting the cessation of flow toward the demonstration well. The flow never fully returned to its predemonstration conditions.

Flow sensor F1 recorded very low horizontal flow velocities before, during, and after the demonstration. While the horizontal velocity never exceeded 0.005 ft/d during the course of the demonstration, changes in flow attributable to the demonstration were nonetheless observed. Before the start of the demonstration, the direction of flow was toward the southwest (240 degrees away from the direction to the demonstration well). When the demonstration started, the direction began to rotate clockwise toward the demonstration well, again reflecting the addition onto the background measurement of a very small flow (a few thousandths of a foot per day) directed toward the demonstration well. This component of flow toward the demonstration well grew steadily for the first 80 days of the demonstration when the pumping rate in the demonstration well was increasing, dropped off during the 6-day interruption around day 80, and then leveled off during the latter part of the demonstration. When the demonstration ended, the flow velocity rotated in a counterclockwise direction away from the demonstration well, reflecting the cessation of flow toward the demonstration well. By 2 months after the termination of the demonstration, the flow had returned to a velocity very close to its predemonstration direction and magnitude.

12.0 Conclusions

After 6 months of operation, the concentration of TCE was reduced significantly in the upper zones of the aquifer and to a lesser extent in the lower zones of the aquifer surrounding the demonstration well. The concentration declines in the upper zones decreased from a high that ranged between 160 to 34 $\mu\text{g/L}$ down to below the regulatory limit of 5 $\mu\text{g/L}$ in most of the monitoring wells around the demonstration well. It was shown that these concentrations could be maintained below the regulatory limit during the demonstration. The rate of TCE decline was variable but, in general, was fastest in the wells nearest the demonstration well. In the lower zones of the aquifer (between 45 and 50 ft below ground surface), the TCE concentration declines were detected in well M3d, the well nearest the demonstration well in which the concentration fell from a pretest concentration of 290 to 173 $\mu\text{g/L}$.

The rate of TCE concentration declines with respect to distance and depth indicated that the flow field may be asymmetrical, a result of the heterogeneous nature of the site geology in both the vertical and horizontal directions. A low-permeability layer at ~44 ft below ground surface appeared to limit the recirculation of the water. TCE concentrations indicated the recirculation zone was at least 10 ft from the well, and semiquantitative mass-balance calculations indicated there may have been recirculation out more than 30 ft from the demonstration well.

Postdemonstration sampling indicated that, in general, there was a notable increase in TCE concentration at each monitoring well completed in the upper part of the aquifer. The monitoring wells in the deep part of the aquifer showed no appreciable change in concentration following the demonstration, with the exception of the intake of the demonstration well and the possible exception of monitoring well M3d.

The flow rates of the system are a function of the submergence-to-lift ratios, injected air volumes, pipe diameters, and formation properties. At the beginning of the demonstration, the pumping rate was limited by the infiltration capacity of the vadose zone; the aquifer could produce more water than what the upper zone could accept. The infiltration capacity increased during the demonstration, possibly the result of increased saturation and the addition of calcium to the reinfiltrating waters that controlled the dispersive clays. The pumping rate increased from ~2.5 gpm in January to > 10 gpm in April, and the flow rates were stabilized at 7 to 8 gpm from May to the end of the test in July.

The airflow rates and the resulting stripping ratios were determined based on the system's configuration. Two basic system configurations were used during the demonstration. The first configuration used 2 blowers and an air-injection depth of ~20 ft. The second configuration was designed to increase the air-to-water ratios and the resulting air-stripping ratios. The second configuration used 3 blowers and the air-injection point was raised to ~8.5 ft. The second configuration increased the air-to-water ratios from ~30 to 54. The stripping rate during the first configuration averaged 89%; that is, 89% of the contaminant was removed per pass through the system. Using three blowers with the second configuration, the stripping ratio averaged 90%.

Better use of the system was made possible by substituting blowers for the air compressor to minimize maintenance and the possibility of injecting compressor oil into the well and adding an eductor pipe that eliminated the potential of injecting air into the formation while maximizing the pumping rate of the system. Of critical importance to the further optimization of the system's performance was the adequate development of both the pumping and injection zones of the well. The upper zone was developed using a combined physical/chemical development. As in agricultural practices, the infiltration rates of the shallow zone were maximized and maintained using a calcium additive. Organic and inorganic precipitation was controlled by running the system in a closed loop and maintaining proper pH by adding carbon dioxide to the injected air stream.

The in-well vapor-stripping system proved successful in removing volatile organic contamination from the groundwater. The system also proved to be very efficient in operation.

13.0 References

- American Society for Testing and Materials. 1994. "Standard Practice for Use of the International System of Units (SI) (the Modernized Metric System)." In *1994 Annual Book of ASTM Standards, Section 14, General Methods and Instrumentation*, Philadelphia, Pennsylvania, pp. 203-236.
- Ballard, S. 1996. "The In Situ Permeable Flow Sensor: A Groundwater Flow Velocity Meter." *Ground Water* 34:231-240.
- Brady, N. C. 1974. *The Nature and Properties of Soils*. MacMillan Publishing Co., Inc. New York. 639 p.
- Comprehensive Environmental Response, Compensation and Liability Act of 1980*, as amended. Public Law 96-510, 94 Stat. 2767, 42 USC 6901 et seq.
- Driscoll, F. G. 1986. *Groundwater and Wells, 2nd Edition*. Johnson Division, UOP, Inc., St. Paul, Minnesota.
- Earth Technology. 1994. *Remedial Investigation Report, Main Base Flight Line Operable Unit No. 1, Edwards Air Force Base, California*. Vol. 1. United States Air Force, Edwards Air Force Base, California.
- Engineering Science. 1988. *Installation Restoration Program, Phase II - Confirmation/Quantification, Stage 3B, for Edwards Air Force Base, California, Final Report, Volumes 1-3*. Prepared for Headquarters Air Force Systems Command, Command Bioenvironmental Engineer (AFSC/SGP), Andrews Air Force Base, Maryland, and United States Air Force Occupational & Environmental Health Laboratory, Technical Services Division, Brooks Air Force Base, Texas.
- Engineering Science. 1989. *RI/FS at Edwards Air Force Base Site 19, Remedial Investigation Report, Volume 1*. Prepared for U.S. Army Corps of Engineers, Omaha District, Omaha, Nebraska.
- Francois, O., T. J. Gilmore, M. J. Pinto, and S. M. Gorelick. 1996. "A Physically Based Model for Air-Lift Pumping." *Water Resources Research* 32(8):2383-2399.
- Gilmore, T. J., and O. Francois. 1996. *Laboratory Testing of the In-Well Vapor-Stripping System*. PNNL-10977. Pacific Northwest National Laboratory, Richland, Washington.
- Gvirtzman, H., and S. M. Gorelick. 1992. "The Concept of In-Situ Vapor Stripping for Removing VOCs from Groundwater." *Transport in Porous Media* 8:71-92.
- Johnson, R. L., P. C. Johnson, D. B. McWhorter, R. E. Hinchee, and I. Goodman. 1993. "An Overview of In Situ Air Sparging." *Ground Water Monitoring and Remediation* 13(4):127-135.

Kabala, Z. J. 1993. "The Dipole Flow Test: A New Single-Borehole Test for Aquifer Characterization." *Water Resources Research* 29(1):99-107.

Oster, J. D., M. J. Singer, A. Fulton, W. Richardson, and T. Prichard. 1992. *Water Penetration Problems in California Soils*. Kearney Foundation of Soil Science, Division of Agriculture and Natural Resources, University of California. 165 p.

Peterson, T. S.; G. H. McCabe, B. R. Brockbank, P. J. Serie, and K. A. Niesen. 1995. *Arid Sites Stakeholder Participation in Evaluating Innovative Technologies: VOC-Arid Site Integrated Demonstration*. PNL-10524. Pacific Northwest Laboratory, Richland, Washington.

Resource Conservation and Recovery Act of 1976, as amended. Public Law 94-580, 90 Stat. 2795, 42 USC 6901 et seq.

Serard, J. L., L. P. Dunnigan, and R. S. Decker. 1976. "Identification and Nature of Dispersive Soils." *Journal of the American Society of Civil Engineers* 101(GT4):11846.

U.S. Environmental Protection Agency (EPA). 1986. *Test Methods for Evaluating Solid Waste, SW-846, Physical/Chemical Methods*. Office of Solid Waste and Emergency Response, Washington, D.C.

White, M. D., M. Oostrom, and R. J. Lenhard. 1995. "Modeling Fluid Flow and Transport in Variably Saturated Porous Media with the STOMP Simulator. No. 1, Nonvolatile Three-Phase Model Description." *Advances in Water Resources* 18:(6)353-364.

White, M. D., and T. J. Gilmore. 1996. *Numerical Analysis of the In-Well Vapor-Stripping System Demonstration at Edwards Air Force Base*. PNNL-11348, Pacific Northwest National Laboratory, Richland, Washington.

Distribution

**No. of
Copies**

**No. of
Copies**

Offsite

S. Ballard, MS 0750
Sandia National Laboratories
1515 Eubank S.E.
Albuquerque, NM 87123

D. Bane
URS Consultants, Inc.
2710 Gateway Oaks Dr., Suite 250 North
Sacramento, CA 95833

A. Bray
EG&G Mound Applied Technologies
P.O. Box 3000
Miamisburg, OH 45343

R. Church
U.S. Department of Energy
P.O. Box 66
Miamisburg, OH 45343

L. Coleman
State of Washington
Department of Ecology
P.O. Box 47600
Olympia, WA 98504-7600

M. Cummings, MS#F604
Los Alamos National Laboratory
P.O. Box 1663
Los Alamos, NM 87545

J. Davis
Zurn Nepco
18578 N.E. 67th Court
Redmond, WA 98052

G. Dawson
EG&G Environmental
Rt. 1, Box 5038-Groverland
Richland, WA 99352

D. Diefendorf
Oak Ridge National Laboratory
P.O. Box 2008
Oak Ridge, TN 37831

2 Earth Technology
100 West Broadway, Suite 5000
Long Beach, CA 90802-4443
ATTN: T. MacHarg
O. Taban

K. L. Fox
State of Ohio
Environmental Protection Agency
401 E. Fifth Street
Dayton, OH 45402

E. Hamilton
722 Victor
Chubbock, ID 83202

T. Hicks
U.S. Department of Energy
Subsurface Contaminant Focus Area
P.O. Box A
Aiken, SC 29808

T. Houk, MS 7615
Lockheed-Martin Energy Systems
P.O. Box 628
Piketon, OH 45661

**No. of
Copies**

**No. of
Copies**

R. Johnson
Oregon Graduate Institute
Department of Environmental Science and
Engineering
P.O. Box 91000
Portland, OR 97291

- 2 Lockheed-Martin Paducah
761 Veterans Avenue
Kavil, KY 42053
ATTN: C. Winkler
W. Richards

P. McCarty
Stanford University
Department of Civil Engineering
Terman Engineering Center
Stanford, CA 94305-4020

T. McKeon
16935 S.E. 39th Street
Bellevue, WA 98008

R. Nichols
Westinghouse Savannah River
Building 773-42A
Aiken, SC 29808

J. O'Kane
State of California
Department of Health Services
Toxic Substances Control
10151 Croydon Way
Sacramento, CA 94105

E. Phillips, EW-923
U.S. Department of Energy
P.O. Box 2001
Oak Ridge, TN 73830

F. Schwartz
Department of Geological Sciences
Mendenhall Laboratory
The Ohio State University
Columbus, OH 43201

B. J. Spargo
Environmental Quality Sciences
Code 6115
Naval Research Laboratory
Washington, DC 20375-5348

- 2 Stanford University
Building 320, Room 118
Stanford, CA 94305-2115
ATTN: S. M. Gorelick
M. J. Pinto

- 2 State of California
Environmental Protection Agency
RWQCB-Lanham, Victorville Branch
15428 Civic Drive, Suite 100
Victorville, CA 93292
ATTN: C. Mitton
R. Flemming

D. Steckel
Air Force Flight Test Center/EMR
70 N. Wolfe Avenue
Edwards AFB, CA 93524-1032

A. Thomas
Armstrong Laboratory
AL/EQM
139 Barnes Drive, Suite 2
Tyndall AFB, FL 32043-5323

- 2 U.S. Environmental Protection Agency
26 W. Martin Luther King Drive
Cincinnati, OH 45268
ATTN: G. Sayles
M. Simon

**No. of
Copies**

**No. of
Copies**

2 U.S. Environmental Protection Agency
Region IX
75 Hawthorne Street
San Francisco, CA 94105
ATTN: R. Simons, H92
R. Russell

J. Yeh
Department of Hydrology
University of Arizona
Tucson, AZ 85721

Onsite

Bechtel Hanford, Inc.

S. Trent XO-37

33 Pacific Northwest National Laboratory

B. Allewan BCO
T. M. Brouns K9-91

J. L. Devary K6-96
R. M. Ecker K6-91
G. R. Holdren K6-81
T. J Gilmore (10) K6-81
H. Kirwan-Taylor SEA
P. E. Long K9-48
G. McCabe SEA
P. J. Mellinger K6-91
T. Naymik BCO
T. Peterson SEA
R. M. Smith K6-96
F. A. Spane, Jr. K6-96
S. Stein SEA
C. K. Thornhill K9-85
M. D. White K9-36
Information Release Office (7) K1-06